SINGLE NANOCRYSTAL SPECTROSCOPY AND PINNED EMISSION OF WHITE LIGHT-EMITTING CADMIUM SELENIDE NANOCRYSTALS

By

Albert Demaine Dukes, III

Dissertation

Submitted to the Faculty of the

Graduate School of Vanderbilt University

in partial fulfillment of the requirements

for the degree of

DOCTOR OF PHILOSPHY

in

Chemistry

May, 2011

Nashville, Tennessee

Approved:

Dr. Sandra J. Rosenthal

Dr. Richard F. Haglund

Dr. David E. Cliffel

Dr. Timothy P. Hanusa

Copyright© 2011 by Albert Demaine Dukes, III

All Rights Reserved

Dedicated

to

my wife, Madeline Jayne Dukes

ACKNOWLEDGMENTS

To my advisor, Dr. Sandra J. Rosenthal, thank you for the chance you gave me by allowing me into your lab. The freedom and independence that you granted me in the lab has allowed me prosper as a researcher. I also want to thank you for allowing me the opportunities to pursue different teaching opportunities and the mentorship you provided in the classroom has made me a much better teacher. The last 6 years have been a lot of fun, they've been a blast.

I would like to thank my Ph.D. committee, Dr. David E. Cliffel, Dr. Richard F. Haglund, and Dr. Timothy P. Hanusa. Your insightful questions helped guide my research. Thank you for all of your help and for being very generous with your time.

To Dr. Jason D. McNeil, you sparked my interest in nanoparticle research when I was a senior at Clemson University. It was on your advice that I came to Vanderbilt, and for that I have to say I am grateful. Dr. Craig Szymanski, thanks for taking me under your wing and allowing me to help you out with a lot of cool research. You made me realize it was possible for research to both interesting and fun.

To Dr. Lloyd Davis and Philip Samson, both of you have been a tremendous help in designing and building the new single nanocrystal spectrometer experiment, I could not have done these experiments without each of you.

I have worked with some tremendous people within the Rosenthal Group. Dr. Danielle Garrett, where should I start? You taught me everything that I know about ultrafast lasers, but more importantly you've been a great friend. I appreciate the

birthday treats that you made and brought into lab, they were awesome. I'll never forget the long hours learning the ropes and the funny stories we shared that got us through them. New students still keep asking me why there are all the decorations you put around my desk when you gave me the key to the laser lab. You were always there to answer any questions I had, even after you graduated, and for that I am eternally grateful. I can only hope that I'll be as good a mentor to my replacement in the laser lab as you were to me.

Dr. Michael Schreuder, thanks for sharing a desk with me for four years. Being able to bounce ideas off of you helped me improve my experiments and made me a better scientist. Dr. Michael Bowers thanks for discovering white-light nanocrystals. Without them I wouldn't have been able to do any of this work. Dr. Nathaniel Smith your ability to explain physics in a simple manner allowed me to better understand the new phenomena I was observing.

Dr. James McBride, you taught how to identify the important questions to drive a project forward. Even after all these years I am still amazed at your ability to get the images I need on an electron microscope. Oleg Kovtun, thanks for being a good friend and occasionally explaining to me what the bio side actually does. Dr. Michael Warnement, thank you for helping me get started with the single nanocrystal experiments. To Joe Keene and Noah Orfield, thanks for replacing me in the laser lab, and good luck.

I would like to thanks the Department of Energy (DEFG0202ER45957) and the National Science Foundation (DMR-0619789) and (EPS-1004083) for the funding which made these experiments possible.

Heather Pillman, I don't think that I would have been a very good chemist if I had never met you, and I know the way pushed me during our junior and senior years is what got me to where I am today, I'll never be able to say thank you enough.

Thanks to my parents, both of whom were teachers, for allowing me to see both the rewarding and challenging side of education. You were always supportive of me whenever I wanted to try something new. Thank you for being there whenever I needed you.

Lastly, Madeline Dukes, my wife, you're definitely the most interesting person I've ever met at an elevator. Thanks for going through all the highs and lows of grad school with me. You were always there to pick me up when experiments weren't working and there to celebrate when they did. I also appreciate you staying late on campus when I had to work late in the laser lab. Being there to help the night the shelf collapsed above the laser, you literally helped me save the laser, and with that you made it possible for me to graduate. Thanks for everything; I couldn't have done it without your support.

TABLE OF CONTENTS

Page

LIST OF TABLES

Page

LIST OF FIGURES

Page

CHAPTER I

INTRODUCTION

1.1 Semiconductor Nanocrystals

Semiconductor nanocrystals are crystals of semiconductor material with dimensions less than 100 nm.[1] When the dimensions of the nanocrystal are reduced below the bulk Bohr diameter, the photogenerated electron-hole pair becomes confined and the nanocrystal exhibits size dependent optical properties.[2,3] CdSe nanocrystals are one of the most widely studied semiconductor nanocrystals because their size-tunable optical properties span the visible spectrum, as shown in Figure 1.1.[4]

Figure 1.1: Photograph of CdSe nanocrystals under room light and UV light. CdSe nanocrystals under room light are shown above. The vials contain nanocrystals ranging from 2-6 nm in diameter. The same vials are shown fluorescing under UV illumination below.

1.1.1 Quantum Confinement

In a bulk semiconductor, when a photon of sufficient energy is absorbed ($h\nu \geq E_g$ (band gap)), an electron-hole pair is formed when the electron is excited from the valence band into the conduction band. The average distance between these charges is given by the bulk Bohr radius and is different for each semiconductor. Quantum confinement arises from a semiconductor material having dimensions physically smaller than the bulk Bohr diameter. Semiconductor nanocrystals gain many of their unique optical properties as a result.[2,3] As the diameter of the crystal is reduced to the bulk Bohr diameter, the energy levels become discrete and boundary conditions are imposed on the wave function of each charge (the electron and the hole), resulting in quantum confinement.[2] Below the bulk Bohr diameter, the diameter of the 1*S* exciton provides an intrinsic measure of the crystal size.[2] The size dependent optical properties can be approximately modeled as a particle in a 1-D box. For a particle confined in a 1-D box the change in energy is related to the inverse square of the box radius given by the following equation:

$$E_n \approx \frac{h^2 n^2}{8mR^2}, \quad n = 1, \ 2, \ 3 \ \ldots \tag{1.1}$$

where h is Plank's constant ($6.626 * 10^{-34}$ J s), m is the mass and R is the nanocrystal radius.

In his foundational work on size dependent properties of nanocrystals, Brus showed a similar relationship between nanocrystal diameter and the band gap.[2] The change from the bulk band gap energy for a semiconducting nanocrystal is given by the following equation:

$$E = \frac{\hbar^2 \pi^2}{2R^2}\left[\frac{1}{m_e} + \frac{1}{m_h}\right] - \frac{1.8e^2}{\varepsilon_2 R} + \frac{e^2}{R}\overline{\sum_{n=1}^{\infty} \alpha_n \left(\frac{S}{R}\right)^{2n}} \tag{1.2}$$

Where E is the change in energy from the bulk band gap, $\hbar$ is the reduced Planck's constant, R is the nanocrystal radius, m_e is the effective mass of the electron, m_h is the effective mass of the hole, ε_2 is the dielectric constant of the semiconductor nanocrystal, α is a constant,[2] and S is the wavefunction for the position of the electron and hole. The first term of Equation 1.2 shows that the change in band gap energy is inversely proportional to nanocrystal radius. As the size of the nanocrystals decrease, the band gap energy increases, resulting in a blue shift of the absorption and fluorescence of the nanocrystals, as shown in Figure 1.1. The second term accounts for the coulombic interaction between the electron and hole, while the third term accounts for the solvation energy loss of the nanocrystal when in solution.

1.2 Ultrasmall Nanocrystals

Ultrasmall nanocrystals have a crystal diameter of 2 nm or less and a majority of their atoms are located on the surface.[5] At these sizes, nanocrystals behave differently than they do at more traditional sizes (larger than 2 nm) and can exhibit unique phenomena, such as quantized growth and intense trap state emission.[6-14] The optical properties of ultrasmall nanocrystals have been previously investigated utilizing both top down[12,15-17] and a bottom up approaches.[7,10,11,13,18]

Early work on ultrasmall CdSe nanocrystals by Soloviev *et al.* reported that the emission spectrum of the these materials, ranging from 0.7-2 nm in diameter, is composed almost exclusively of trap state emission.[13] The extremely high surface to volume ratio for nanocrystals means that the surface states, which are often neglected in larger nanocrystals, play a dominate role in determining the emission properties of

ultrasmall nanocrystals. Soloviev also observed that when their ultrasmall nanocrystals were continuously illuminated at low temperature (20 K), quenches over time. However, when the quenched samples were warmed to 200 K in the dark, and then cooled back down to 20 K, the emission partially recovered.[13] The quenching of the emission is attributed to photochemical cleavage of the surface passivating ligand.[13] Removal of the surface ligand introduces a nonradiative trap site, which quenches the emission. The loss of surface ligands is responsible for the incomplete recovery of fluorescence intensity. The other mechanism by which the nanocrystal emission is quenched is that the nanocrystals become charged in a manner analogus to nanocrystal blinking.[13]

Landes *et al.* were one of the first to report optical phenomena in ultrasmall CdSe nanocrystals, which differed from that of traditionally sized CdSe nanocrystals.[17] Landes observed that when traditional CdSe nanocrystals were treated with the hole acceptor n-butylamine, the fluorescence quenches with increased amine concentration, but the fluorescence lifetime remained unchanged.[19] However, when this experiment was repeated on ultrasmall nanocrystals, a decrease in the fluorescent lifetime was observed in addition to the fluorescence quenching.[12] Besides the change in the fluorescent lifetime, Landes noted that n-butylamine would etch ultrasmall nanocrystals to smaller sizes, resulting in a blueshift of the band edge absorption,[16,17] while the band gap of the traditionally sized CdSe nanocrystals was unaltered.[19]

The reports by Landes *et al.* noted the presence of an isobestic point in the absorption spectrum as n-butylamine was added to the ultrasmall CdSe nanocrystals.[15,17,20] The isobestic point shows that there are two species which are in equilibrium with each other. This effect was similar to the pressure induced phase

transition observed by Tolbert and Alivisatos,[21] which suggests the isobestic point would be the equilibrium point for two different crystal structures.[17] Landes also concluded that the amine binding to the ultrasmall nanocrystal surface is an exothermic process which releases sufficient energy to break a Cd-Se bond.[17] That the ultrasmall CdSe nanocrystals stabilize to a size corresponding to a band edge absorption at 414 nm is explained by the presence of a uniquely stable magic-size structure.[17]

1.2.1 Magic-Size Nanocrystals

Magic-sized nanocrystals are a special class of ultrasmall nanocrystals. Magic-sized nanocrystals are hypothesized to have a unique crystal structure which only allows certain stable sizes to exist.[6-9,22,23] Modeling experiments have proposed that the stability of magic-size nanocrystals results from a closed-cage crystal structure, similar to that of fullerenes, as shown in Figure 1.2. The possible structure consists of alternating 4 and 6 member rings. This possible structure differs significantly from the commonly observed wurtzite or zinc blende structure for CdSe nanocrystals. This possible structure implies stable crystal structures in nanomaterials which are not observed in the bulk material could exist.

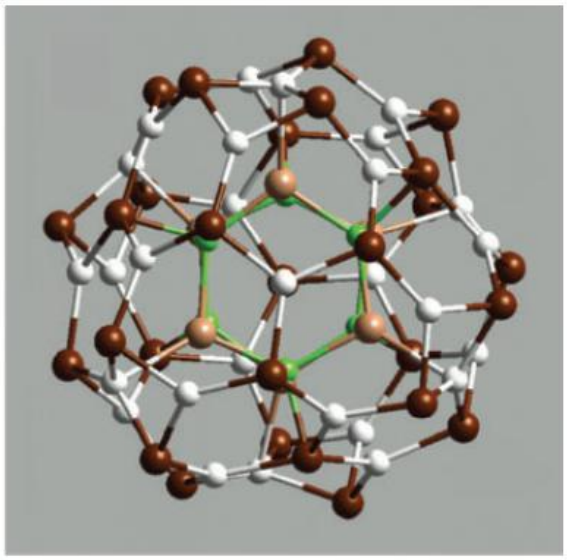

Figure 1.2: Possible structure of magic-sized CdSe nanocrystals. The modeling by Kasuya *et al.* have proposed the above closed-cage structure for magic-sized CdSe nanocrystals.[8]

Magic-sized nanocrystals are also a promising material for commercial application because their well defined number of atoms results in nanocrystals with nearly identical optical properties.[7] Magic-sized nanocrystals have been successfully shelled with ZnS and incorporated into a prototype light emitting diode.[7] In addition to their potential application is light emitting diodes, the small diameter of magic-sized nanocrystals makes them an attractive candidate for development as a biological probe. Magic-size nanocrystals are well below the 5 nm diameter necessary to clear the body,[24] and they have recently been reported with a narrower emission spectrum than traditional nanocrystals.[6] This extremely narrow emission spectrum coupled with a small probe size would be ideal for multi-target labeling studies.

1.2.2 White-Light Emitting CdSe Nanocrystals

In 2005, white-light emission from ultrasmall CdSe nanocrystals was reported for the first time.[10] White-light nanocrystals have band edge absorption at 414 nm, along with a narrow size distribution.[10,18] This material also has a broad emission spectrum which spans the visible spectrum, as shown in Figure 1.3. The broad emission spectrum has been shown to be the result of trap state emission, though the exact trap states responsible for each peak in the emission spectrum have yet to be determined.[5] Scanning transmission electron micrographs of the white-light nanocrystals indicate that the crystals have a wurtizite crystals structure, similar to larger CdSe nanocrystals which are passivated with alkylphosphonic acid surface ligands.[5,18]

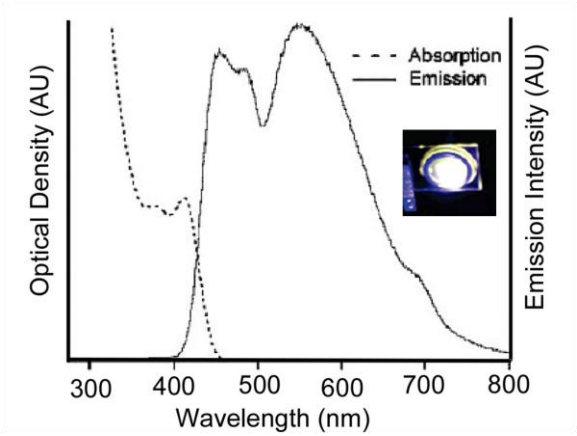

Figure 1.3: Absorption and emission spectra of white-light CdSe nanocrystals. The narrow absorption spectrum of white-light emitting CdSe nanocrystals is shown in the dashed curve. The broad emission spectrum has peaks at 440 nm, 488 nm, and 550 nm. The inset shows a film of white-light emitting CdSe nanocrystals under excitation from a UV laser.

Because the white-light nanocrystals have an emission spectrum similar to sunlight they are an ideal material for use as the emitting layer in a solid-state lighting device. Prototype photoluminescent devices with the white-light nanocrystals dispersed

in the commercial polymer nanoparticle dispersion matrix, have recently been demonstrated.[25] This polymer protects from oxidation without altering the emission spectrum. Electroluminescent devices based on white-light nanocrystals have also been constructed.[26] While the white light-emitting CdSe nanocrystals have been employed in devices, no previous studies have been able to determine if the individual nanocrystals emit white light, or if it is simply an ensemble effect.

1.3 History of Single Nanocrystal Spectroscopy

Single nanocrystal spectroscopy was first performed by Nirmal *et al.* and revealed phenomena not observed in ensemble measurements.[27] The first of these properties is fluorescence intermittency, or blinking. Observation of blinking provides a quick and simple method for ensuring that an individual fluorophore is being observed.[27-39] The statistics of nanocrystal blinking has been studied by Kuno *et al.*[28,29] They determined that the duration of the ON time has a quadratic dependence on excitation power; however, the OFF time is independent of excitation power.[28,29] Kuno *et al.* measured an inverse power-law distribution of the ON and OFF times.[28,29]

It was also observed that upon continuous illumination, the emission spectrum of an individual CdSe nanocrystal will blue shift.[27,40] The blue shift is the result of photooxidation at the nanocrystal surface. As the nanocrystal photooxidizes, the effective radius of the nanocrystal decreases.[27] The decreased radius results in an increased band gap of the nanocrystal.[2] The emission from an individual nanocrystal is also narrower than the ensemble fluorescence measurement.[27,41,42] The theoretical full

width at half maximum intensity for a semiconductor nanocrystal at room temperature is ~100 meV, which would yield an emission spectrum 2-3 times narrower than the ensemble spectrum.[41,43,44] While the current strategies for nanocrystal synthesis yield highly monodisperse samples, there are still slight variations in crystal diameter within the sample which results in nanocrystals with slightly different diameters.[45] Because the nanocrystal's optical properties are related to crystals size,[2] slight variations in size within a sample will broaden the ensemble spectrum.

1.4 Overview

This dissertation examines the optical properties of ultrasmall CdSe nanocrystals and reports on the discovery of new optical phenomena. Chapter I provides a general overview of quantum confinement in semiconductor nanocrystals, single-nanocrystal spectroscopy, and ultrasmall nanocrystals. Two special types of ultrasmall nanocrystals, magic-sized nanocrystals and white-light emitting nanocrystals, are specifically addressed. Chapter II details the experimental methods for synthesizing white-light emitting CdSe nanocrystals, magic-sized CdSe and CdTe nanocrystals, as well as the surface ligand exchanges that replace the alkylphosphonic acid ligands with dodecanethiol, pyridine, and oleic acid. Additionally, the methods used to prepare ultrasmall nanocrystals for characterization by UV-visible absorption spectroscopy, fluorescence spectroscopy, photoluminescence excitation spectroscopy, and transmission electron microscopy are discussed.

Chapter III details the discovery of pinned, or size-independent, emission in white-light emitting CdSe nanocrystals. The wavelength of the first emission feature for ultrasmall nanocrystals with a diameter ranging from 1.3-2.0 nm, and for larger nanocrystals up to 4 nm in diameter, is measured. This study determined that the emission spectrum becomes pinned when the nanocrystals have a diameter of 1.7 nm or smaller. At nanocrystal diameters larger than 1.7 nm the broad emission collapses. Post-preparative ligand exchanges with a thiol, carboxylic acid, and pyridine determine that the pinned emission results from a surface-ligand trap state. It is proposed that this trap state has a fixed energy above the conduction band of larger nanocrystals but within the band gap of ultrasmall CdSe nanocrystals. Chapter IV investigates the use of diisooctylphosphinic acid as a surface ligand for ultrasmall CdSe and CdTe nanocrystals. The use of diisooctylphosphinic acid instead of an alkylphosphonic acid results in magic-size nanocrystals which display a quantized growth spectrum. The use of diisooctylphosphinic acid allows for the synthesis of larger magic-sized nanocrystals than previously reported synthetic methods. Three distinct magic-sizes of CdSe and two distinct magic-sizes of CdTe nanocrystals were synthesized. Transmission electron micrographs indicate a morphological change as the CdSe and CdTe magic-size nanocrystals grow from the smallest size to the next largr size. Chapter V examines the fluorescence spectrum of an individual white-light emitting nanocrystal and describes the construction of the single nanocrystal fluorescence spectrometer. There are two possible explanations for the white-light emission spectrum: either every nanocrystal emits all three peaks, or are there three distinct populations, one emitting blue, a second emitting green, and a third emitting red. To answer this question, a single-nanocrystal

fluorescence spectrometer was constructed and the emission spectra of 252 individual nanocrystals were measured. It was determined that each white-light emitting nanocrystal individually emits white light on the timescale of the measurement (50 ms integration time). This result means that each white-light nanocrystal contains all the trap states necessary to emit white light.

CHAPTER II

EXPERIMENTAL METHODS

2.1 Experimental Overview

The procedures for synthesizing white light-emitting CdSe nanocrystals as well as magic-sized CdSe and CdTe nanocrystals are described in detail. The analytical techniques used to characterize the synthesized nanocrystals are also described. The sample preparation techniques for the single nanocrystal spectroscopy experiments are described, as well as the operation of the instrument.

2.2 Synthesis of CdSe Nanocrystals with Alkylphosphonic Acid Surface Ligands

A photograph of the synthetic setup is shown in Figure 2.1. CdSe nanocrystals were synthesized with dodecylphosphonic acid as the surface ligand by following previously published procedures.[46] Briefly, 1mmol of CdO was combined with 2 mmol of dodecylphosphonic acid, 7 g trioctylphosphine oxide (TOPO, Aldrich, 90%), and 3 g HDA in a three-neck flask. The flask was fitted with a rubber septum, temperature probe, and bump trap. The reaction mixture was purged with argon to 140 °C, the purge needle was removed, and the reaction mixture was heated under an argon atmosphere to 330 °C. When the reaction mixture was colorless, 5 mL of 0.2 M Se:TBP was injected. The nanocrystal solution was heated at 280 °C until the desired size was reached. Nanocrystal growth was monitored by UV-Vis absorption spectroscopy.

The CdSe nanocrystals were isolated by precipitation with methanol and collected by centrifugation. The colored pellet was then dispersed in octanol, and the unreacted precursors were collected by centrifugation. The nanocrystals were then precipitated from the octanol solution by the addition of methanol and collected by centrifugation. The nanocrystal pellet was then dispersed in toluene for analysis.

Figure 2.1: Photograph of the nanocrystals synthesis setup.

2.3 Synthesis of Ultrasmall CdSe Nanocrystals

CdSe nanocrystals with a band edge absorption ranging from 375-373 nm (1.3-3.7 nm in diameter) capped with an alkyl phosphonic acid[47] were synthesized similar to the procedure reported by Bowers *et al.*[10] Tri-*n*-butylphosphine (TBP) (tech grade 97%–99%), selenium shot (200 mesh), cadmium oxide _99.99%_ triethylphosphite, dodecylbromide, octylbromide, hexadecylbromide (all reagent grade), and hexadecylamine (HDA) (tech grade 90%) were purchased from Aldrich or Strem and used as delivered. The alkyl phosphonic acids were synthesized according to standard procedures.[48,49] The reactive cadmium precursor was prepared by combining 20 g of

HDA, 2 mmol of CdO, and 4 mmol of the phosphonic acid into a three-neck flask that was fitted with a temperature probe, bump trap, and a rubber septum. The phosphonic acids used in these experiments were either octylphosphonic acid, dodecylphosphonic acid, or hexadecylphosphonic acid. The reaction mixture was stirred and purged with argon until the reaction reached 150 °C. The temperature was then raised to 320 °C and stirred until the solution became clear and colorless. Once the solution was colorless, 10 ml of 0.2M Se:TBP solution was injected. The reaction was halted with a 20 ml injection of butanol followed by cooling with compressed air until the temperature dropped below 100 °C. The nanocrystals were cleaned by precipitation with methanol and collected by centrifugation. The yellow pellet was then dispersed in hexanol and centrifuged to collect the undissolved HDA. The nanocrystals were then precipitated from the hexanol by the addition of methanol and collected by centrifugation.

The cleaned nanocrystals were dispersed in hexanes for ligand exchange. 5 ml of 0.5 μM nanocrystal solution was added to 15 ml of pure ligand, for ligand exchange with pyridine and oleic acid. These solutions were allowed to stir overnight at room temperature. The nanocrystals were then diluted with hexanes for spectroscopic measurements. For ligand exchange with dodecanethiol, three drops of dodecanethiol were added to a cuvette of ultrasmall nanocrystals in hexanes (0.17 μM) and stirred. Static absorption and emission spectra were obtained using a Cary Bio 50 UV-visible spectrometer and an ISS PC1 photon counting fluorometer, respectively.

2.4 Synthesis of Magic-Size CdSe Nanocrystals

CdSe nanocrystals were synthesized as previously reported,[50] with the exception that diisooctylphosphinic acid was used as the capping ligand, instead of a phosphonic acid. Briefly, 1 mmol of CdO (99.99 %, Strem) and 10 g of hexadecylamine (HDA, 98 %, Aldrich) were combined in a threeneck flask that was fitted with a temperature probe, bump trap, and rubber septum. The reaction mixture was stirred and purged with argon until the mixture reached 150 °C. Then 2 mmol of diisooctylphosphinic acid (90%, Aldrich) was injected and the temperature was then raised to 310 °C. Once the solution was colorless, 5 mL of 0.2 M Se:tributylphosphine solution (Se 200 mesh, Strem; TBP, tech grade 97-99 %, Aldrich) was injected, initiating the formation of CdSe nanocrystals. As soon as a yellow color was observed, the reaction was halted with a 20 mL injection of butanol, followed by cooling with compressed air until the temperature dropped below 100 °C.

2.5 Synthesis of Magic-Sized Nanocrystals in TOPO

One1 mmol of CdO was combined with 10 g of n-tri-octylphosphine oxide (TOPO, 90% or 99%, Aldrich) in a three-neck flask and fitted with a rubber septum, bump trap, and temperature probe. The mixture was purged with argon until a temperature of 150°C was reached. Then 2 mmol of diisooctylphosphinic acid was injected and the temperature was raised to 310°C. Once the solution was colorless, 5 mL of 0.2M Se:TBP was injected, causing the formation of CdSe nanocrystals. The reaction was halted with a 20 mL injection of butanol, followed by cooling with compressed air until the temperature dropped below 100°C. For nanocrystal growth the reaction was

reheated to 150°C, and the butanol was boiled off. Growth was monitored by UV-visible absorption spectroscopy.

2.6 Synthesis of Magic-Size Nanocrystals in Non-Coordinating Solvent

One mmol of CdO was combined with 10 mL octadecene (ODE, 90% Aldrich) in a three-neck flask and fitted with a rubber septum, bump trap, and temperature probe. The mixture was purged with argon until a temperature of 150°C was reached. Then 2 mmol of diisooctylphosphinic acid was injected and the temperature was raised to 310°C. Once the solution was colorless, 5 mL of 0.2M Se:TBP was injected, causing the formation of CdSe nanocrystals. The reaction was halted with a 20 mL injection of butanol, followed by cooling with compressed air until the temperature dropped below 100°C. For nanocrystal growth the reaction was reheated to 150°C, and the butanol was boiled off.

Growth was monitored by UV-visible absorption spectroscopy.

2.7 Synthesis of Magic-Sized Nanocrystals in a Mixed Solvent System

One mmol of CdO was combined with 5 g TOPO and 5 g of HDA in a three-neck flask and fitted with a rubber septum, bump trap, and temperature probe. The mixture was purged with argon until a temperature of 150°C was reached. Then 2 mmol of diisooctylphosphinic acid was injected and the temperature was raised to 310°C. Once the solution was colorless, 5 mL of 0.2M Se:TBP was injected, causing the formation of CdSe nanocrystals. The reaction was halted with a 20 mL injection of butanol, followed

by cooling with compressed air until the temperature dropped below 100°C. For nanocrystal growth, the reaction was reheated to 150 °C and the butanol was boiled off. Growth was monitored by UV-visible absorption spectroscopy.

2.8 Cd-Rich Synthesis of Magic-Sized Nanocrystals

One mmol of CdO was combined with 10 g of HDA in a three-neck flask fitted with a bump trap, rubber septum, and temperature probe. The reaction was purged with argon to 150 °C. 2 mmol diisooctylphosphinic acid was injected into the reaction flask. The temperature was the raised to 310 °C. Once the solution was colorless, 1 mL of 0.2MSe:TBP was injected, causing the formation of CdSe nanocrystals. The reaction was halted with a 20 mL injection of butanol followed by cooling with compressed air until the temperature dropped below 100 °C. For nanocrystal growth, the reaction was reheated to 150 °C and the butanol was boiled off. Growth was monitored by UV-visible absorption spectroscopy.

2.9 Se-Rich Synthesis of Magic-Size Nanocrystals

One mmol of CdO was combined with 10 g of HDA in a three-neck flask and fitted with a bump trap, rubber septum, and temperature probe. The reaction was purged with argon to 150 °C. 2 mmol diisooctylphosphinic acid was injected into the reaction flask. The temperature was the raised to 310 °C. Once the solution was colorless, 3.3 mL of

1.5 M Se:TBP was injected, causing the formation of CdSe nanocrystals. The reaction was halted with a 20 mL injection of butanol followed by cooling with compressed air

until the temperature dropped below 100 °C. For nanocrystal growth the reaction was reheated to 150 ^{o}C and the butanol was boiled off. Growth was monitored by UV-visible absorption spectroscopy.

2.10 Synthesis of Magic-Size CdTe Nanocrystals

CdTe nanocrystals were synthesized under the same reaction conditions as the CdSe nanocrystals. Briefly, 1 mmol of CdO and 10 g of HDA were combined in a three-neck flask that was fitted with a temperature probe, bump trap, and rubber septum. The reaction mixture was stirred and purged with argon until the mixture reached 150 °C. Then 2 mmol of diisooctylphosphinic acid was injected and the temperature was raised to 310 °C. Once the solution was colorless, 5 mL of 0.2 M Te:TBP solution (Te 200 mesh, Acros) was injected, initiating the formation of CdTe nanocrystals. The reaction was halted with a 20 mL injection of butanol, followed by cooling with compressed air until the temperature dropped below 100 °C. While the reaction for the magic-sized CdSe nanocrystals was quenched at the first sign of the solution turning yellow, this was not possible for the CdTe nanocrystal reaction because the Te:TBP solution is naturally yellow. Instead the reaction mixture was allowed to react for 3 seconds before it was quenched with the butanol injection.

2.11 Growth and Isolation of Magic-Size Nanocrystals

Zero minutes of growth represents the time at which the reaction solution had cooled below 100 °C, the initial aliquot (0.3 mL nanocrystals solution diluted with 3 mL

of toluene) was withdrawn from the solution, and the absorption spectrum was measured. The heating mantle was then reapplied to the flask, and the temperature was raised to 150 °C. We began measuring the growth time as soon as the heating mantle was reapplied. The growth was monitored by UV-Vis absorption spectroscopy on a Cary Bio 50 UV-visible spectrometer. When the nanocrystals reached the desired size, growth was halted by cooling the flask with compressed air and adding hexanes to dissolve the nanocrystals. The nanocrystals were cleaned by first precipitating them via the addition of methanol and collecting them by centrifugation. The nanocrystals were then redissolved in hexanes, and all undissolved material was collected by centrifugation. The nanocrystals remained dispersed in hexanes for analysis and electron microscopy. All photoluminescence measurements were made on an ISS PC1 single photon counting fluorimeter. Transmission electron microscopy (TEM) was performed on a Phillips CM20 operating at 200 kV.

2.12 Ligand exchange of Dodecylphosphonic Acid for Diisooctylphosphinic Acid

CdSe nanocrystals capped with dodecylphosphonic acid were synthesized with a band edge absorption of 541 nm as described previously.[51] Diisooctylphosphinic acid was diluted with toluene to a concentration of 1 M. The dodecylphosphonic acid capped nanocrystals were diluted to a concentration of 15 mM by the addition of toluene. A 4 mL aliquot of these nanocrystals was added to 4 mL of the 1 M diisooctylphosphinic acid ligand in a glass vial. The resulting solution was stirred and heated to 80 ºC to drive the ligand exchange. The solution was heated for 24 hours.

2.13 Operation of the Single Nanocrystal Spectrometer

The light source for the single nanocrystal spectrometer is the frequency doubled fundamental output from a Ti: Sapphire laser. Mode-locking the laser and unblocking the β-BBO crystal will allow the frequency doubling necessary for the generation of 400 nm light. The residual 800 nm light is removed by a series of short pass filters. There are several irises which are in the beam path to ensure the day to day alignment of the excitation beam. While not shown in Figure 5.2, there are a series of beam splitters which split the incoming 400 nm pulse into four parts. For the single nanocrystal spectrometer, only the straight through path of these interferometers is utilized, all other paths are blocked with beam blocks.

A remote control mechanical shutter is present after the beam splitters, but before the Köhler lens. This shutter is to remain closed except when collecting a fluorescent image or focusing to prevent photobleaching of the sample. A drop of deionized water must be added to the objective because it is a water immersion objective. Carefully place a coverslip on the sample stage, and adjust the correction collar for the correct thickness of the coverslip used. The correction collar is adjustable for glass thickness ranging from 130-210 μm. Apply the metal cover over the coverslip to prevent laser light which is not absorbed from scattering into the room. The simplest way to focus the microscope is to open the mechanical shutter and adjust the z-axis of the piezo stage until the back reflection is in focus on a business card before the third beam splitter. Close the mechanical shutter, and apply the sample as described as section 2.14.

The camera software is controlled by the Andor iXon software program. When the program is open you should hear the camera shutter open. The camera shutter can be opened or closed by the user under the hardware menu. The same menu has the temperature controls. The software will remember the temperature settings last used to cool the camera, so it is not necessary to set this every imaging session. To current camera temperature is displayed in the lower left hand corner of the screen and it red when the camera is above the set temperature and changes to blue when the desired temperature is reached. The camera shutter should be closed whenever the camera is not in use to avoid damaging the CCD.

The acquisition menu is used to input the image collection settings described in section 2.14.1. The user must input this setting at the beginning of each day's imaging session. The current screen for acquiring an image will always be named Acquisition 0. To observe the sample under the programmed settings without collecting the data the user should click on the video camera icon on the toolbar. This operates the camera in free run video, but does not save the images. This mode is useful to find focus and samples to image. To begin collecting and saving images the user should press the camera icon located next to the video camera icon. At the end of the collected movie the user should close the mechanical shutter on the table and then save the file, **the collected files do not save automatically.**

The Andor software saves images as a .sif flie extension. In order to convert these files to other types such as .tiff the user must use the "batch conversion" command under the File menu. Using the example of the .tiff file extension, this command will convert each frame of the collected movie into its own .tiff file. Therefore a 1000 frame

movie is converted into 1000 individual .tiff files, and can then be analyzed using image analysis software of the user's choice.

2.14 Sample Preparation for Single-Nanocrystal Spectroscopy

The concentration of the stock white-light nanocrystal solution was determined by UV-visible absorption spectroscopy. The extinction coefficient was calculated using the equations of Yu *et al*.[45] Aliquots of the stock solution were then diluted with hexanes to a concentration ranging from 20-70 nM. The resulting solution was then sonicated for 30 minutes to break up any possible aggregates that formed during the precipitation steps of the clean-up procedure. A 200 μm thick fused silica coverslip (Structure Probe Inc, 01015-AB) was plasma cleaned with an air plasma to ensure a clean surface. A drop of the sonicated nanocrystal solution was added to the coverslip and the hexanes allowed to evaporate.

2.14.1 Spectral Imaging Conditions

With the Köhler lens providing wide-field illumination, the experimental geometry allows for the simultaneous collection of many nanocrystal spectra in a single measurement. For such measurements, the EM-CCD camera was thermo-electrically cooled to −50 °C and the exposure time was set to 50 ms per frame. A low laser irradiance (~200 Wcm^{-2}) and high electron multiplier gain (500×) were used to reduce photo-bleaching. Movies were collected with the camera operating in frame-transfer kinetic mode with 1,000 or 10,000 frames in the series.

CHAPTER III

PINNED EMISSION OF ULTRASMALL CADMIUM SELENIDE NANOCRYSTALS

3.1 Optical Properties of Ultrasmall Nanocrystals

Ultrasmall semiconductor nanocrystals, those with a diameter of less than 2 nm, have become a recent topic of interest.[10,14,20,52-57] A primary focus of this research has been on determining the origin of the broad emission in ultrasmall CdSe nanocrystals. Work by Puzder *et al.* concludes that the emission is from a surface state,[56] while work by Lee *et al.* suggests the emission arises from a state in the 5p/5s state in the conduction band that is unaffected by quantum confinement.[57] The intense study of these nanocrystals has been driven by their uniquely broad white-light emission. With the recent incorporation of this material into solid state lighting devices,[25] it is necessary to understand the nature of the emitting states in order to enhance the quantum yield of the material.

3.1.1 Origin of the Stokes Shift in Semiconductor Nanocrystals

Ultrasmall nanocrystals have a nonresonant Stokes shift of greater than 20 nm, as compared to larger nanocrystals, which have a 10–15 nm nonresonant Stokes shift.[58] The origin of the Stokes shift in larger CdSe nanocrystals was investigated by Efros *et al.*[59] and Kuno *et al.*[60] The nonresonant Stokes shift is too large to be explained by exciton-

phonon coupling alone.[59] While it is possible to explain the Stokes shift as a surface effect caused by recombination of weakly overlapping surface carriers, a more complete model is produced when the ground exciton is an optically forbidden state split from the first optically active state by the electron-hole exchange interaction.[59] In the dark exciton model, Kuno *et al.* calculated the exciton fine structure to reveal that the band edge absorption results from the mean of three energy levels: $\pm 1^L$, $\pm 1^U$, and 0^U weighted for oscillator strength.[60] The Stokes shift is the difference between the mean of these three states and the $\pm 2^L$ dark exciton.[59,60] This model predicts that the nonresonant Stokes shift for larger nanocrystals is ~25 meV (10–15 nm) and will increase as the diameter of the nanocrystal decreases.

3.1.2 Theoretical Calculations and Experimental Measurements on Ultrasmall CdSe Nanocrystals

A recent theoretical study by Puzder *et al.* investigated the origin of the band gap in ultrasmall CdSe nanocrystals. They performed *ab initio* calculations on the electronic structure, utilizing a plane wave implementation of density functional theory, which showed that the size dependent band gap in CdSe nanocrystals resulted from a structural relaxation at the surface.[56] Further, their work indicated that the surface passivating ligand has a negligible effect on the band gap of CdSe. The work of Puzder *et al.* is also interesting because their models of the band gap for CdSe show a consistent ~1 eV blueshift from the bulk value for all the ultrasmall sizes they studied. The implication of this is that at smaller sizes the absorption and emission spectra should stop blueshifting and be pinned at 2.8 eV (443 nm).

X-ray absorption measurements were performed by Lee *et al.* on CdSe nanocrystals, which showed that at ultrasmall sizes the conduction band minimum would become pinned.[57] The work of Lee *et al.* indicated that the Cd 5*s* /5*p* state was unaffected by quantum confinement, and that at ultrasmall sizes this hybridized state becomes the bottom of the conduction band as the Cd 5*s* state moves to higher energy due to quantum confinement. However, Lee *et al.* were unable to distinguish between bulk and surface states and could not determine the origin of the pinning.

3.1.3 White-Light Nanocrystals as the Model System for Ultrasmall Nanocrystals

As first discovered by Bowers *et al.*,[10] monodisperse ultrasmall CdSe nanocrystals can be synthesized, which have a uniquely broad band, white-light emission (Fig. 3.1). These nanocrystals are an ideal candidate on which to test the pinning prediction of Puzder *et al.* and Lee *et al.* because they are in the size regime at which Lee *et al.* predicts pinning should occur. Also, the first feature of their emission spectrum is near the energy predicted by the model of Puzder *et al.* The larger-than-expected Stokes shift suggests that this peak is not the result of band-edge recombination and is consistent with the predictions of the model proposed by Kuno *et al.* and Efros *et al.* We report the observation of the pinning of the emission spectrum in ultrasmall CdSe nanocrystals. We observe that the first emission feature no longer blueshifts with the continued blueshift in the absorption spectrum once the nanocrystals reach a diameter at or below 1.7 nm. Post preparative ligand exchanges indicate that a surface state related to the alkyl phosphonic acid on the surface causes the pinning.

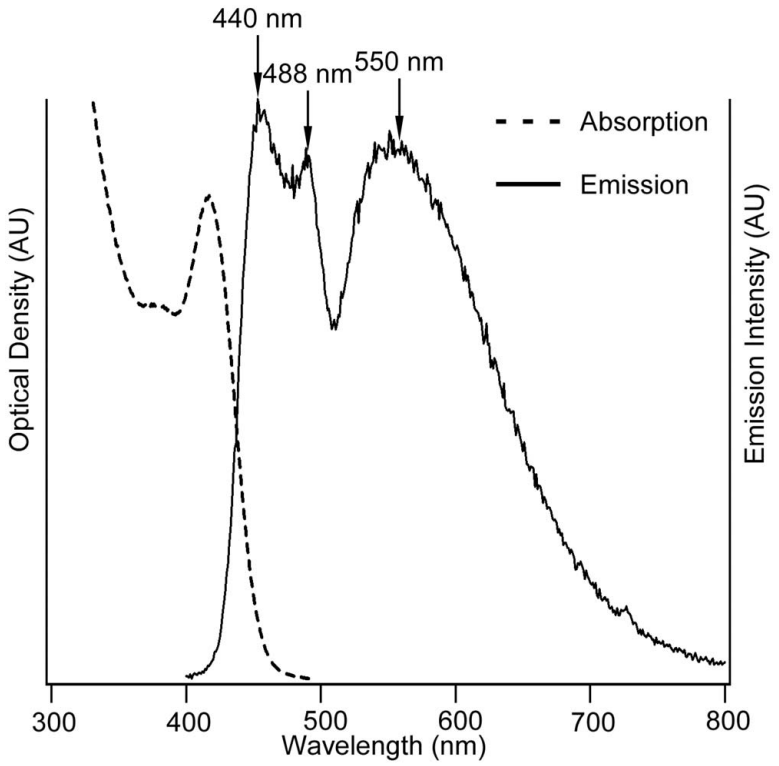

Figure 3.1: Absorption and labeled emission spectrum for white-light CdSe nanocrystals. The absorption spectrum (dashed line) of the ultrasmall, 1.6 nm in diameter, nanocrystals indicates a narrow size distribution. These nanocrystals have broad spectrum, white-light emission (solid line).

3.2 Observation of Pinned Emission

The bluest peak in Fig. 3.1 (440 nm) appears to be band edge recombination, while the remaining two peaks suggest surface-state recombination. However, if the first peak is band-edge recombination, it would be expected to blueshift as the size of the nanocrystals is reduced, in accordance with a quantum confinement; however, this was not observed. Instead, when the nanocrystal's diameter reached 1.7 nm, the position of the first peak remained constant as the size of the nanocrystals was decreased. This is clearly displayed in Fig. 3.2, where the position of the first emission peak was plotted versus the position of the first absorption peak (this was related to nanocrystal diameter

using the sizing fit function developed by Yu *et al.*)[45] While Yu *et al.* were unable to image nanocrystals in this size regime with electron microscopy, they were sized using x-ray diffraction. The line on each graph represents the trend of the nanocrystal emission blue shifting with a blue shift in the absorption. Pinning of the emission spectrum occurs when the position of the first emission feature deviates from this trend. This is observed when the band edge absorption is below 420 nm.

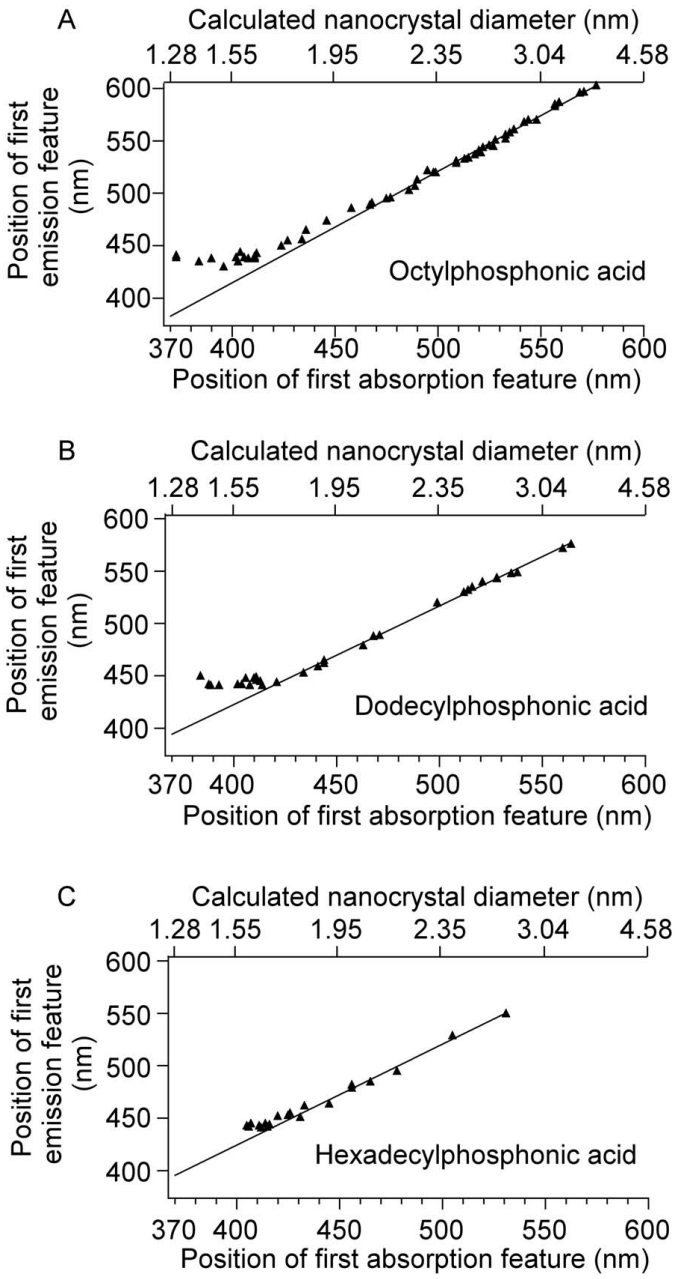

Figure. 3.2: Pinned emission spectrum for CdSe nanocrystals. The position of the first emission feature is plotted against the position of the first absorption feature for CdSe nanocrystals passivated with (A) octylphosphonic acid, (B) dodecylphosphonic acid, and (C) hexadecylphosphonic acid. In all cases, when the band edge absorption wavelength is below 420 nm, corresponding to nanocrystals less than 1.72 nm in diameter,[45] the first emission feature is pinned at approximately 440 nm. The line on each graph represents the trend of blueshifting emission with a blueshift in the absorption. The emission spectrum remains broad and unchanged at nanocrystal sizes below 2 nm.

Our observation of the pinned emission confirms the predictions made by Lee *et al.* that CdSe nanocrystal emission would become pinned when its diameter is less than 2 nm.[57] In their work, it was proposed that the conduction band minimum would become pinned at sizes below 2 nm in diameter due to the Cd 5*s* state moving to a higher energy than the Cd 5*p*/5*s* state, which is not affected by quantum confinement.[57] They showed that the parabolic nature of the Cd 5*s* state makes it highly influenced by quantum confinement, while the hybridized Cd 5*p*/5*s* state is flat and localized, making the hybridized state unaffected by quantum confinement. This would show up experimentally as a lower limit for the onset of band edge absorption. However, this mechanism does not account for the pinning we have observed, since it is clear from Fig. 3.2 that the band edge absorption continues to blueshift. If the conduction band minimum were pinned because the Cd 5*p*/5*s* state is unaffected by quantum confinement, then the band edge absorption would stop blueshifting at smaller sizes, but this is not observed. Instead we observed a continuing blueshift in the band edge absorption, while the first emission feature is pinned.

3.3 Effect of the Surface Ligand on the Emission Spectrum

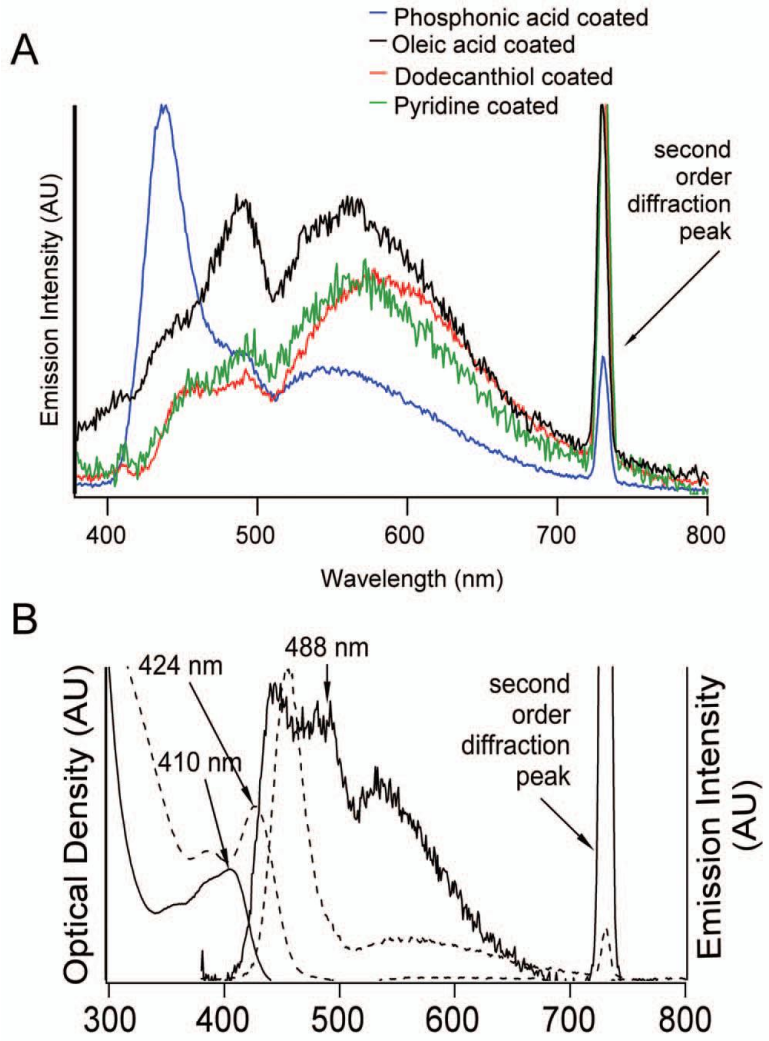

Figure. 3.3: Effect of surface ligand and size on white-light emission spectrum. (A) The emission from nanocrystals, 1.6 nm in diameter, synthesized in octylphosphonic acid is shown in blue. After a ligand exchange with dodecanthiol (red), oleic acid (black), and pyridine (green), the emission from the feature at 440 nm is quenched. (B) The absorption and emission of nanocrystals within the pinning regime (solid) and outside the pinning regime (dashed) is shown. The emission feature at 488 nm is present in the nanocrystals within the pinning regime, but is absent in the larger nanocrystals.

Although the work of Puzder *et al.* suggested that the surface ligand had no affect on the band gap of CdSe, it did indicate that the ligand could affect the quantum yield of the nanocrystal.[56] Several post preparative ligand exchanges were performed to determine

if a different surface passivation would affect the surface state leading to the emission at 440 nm. To test this, the alkyl phosphonic acid was replaced with either dodecanethiol, pyridine, or oleic acid ligands (Fig.3.3A), all of which bind to the surface Cd atoms. In all cases, the emission feature at 440 nm is quenched when the alkyl phosphonic acid is replaced by a different ligand. The emission feature that appears slightly redshifted of 400 nm is the result of Raman scattering from the hexanes used to disperse the nanocrystals.[61] As the phosphonic acid ligands are replaced by new ligands, it is likely that the surface of the nanocrystal becomes altered leading to the elimination of the surface state responsible for the emission at 440 nm. In previous work on etching nanocrystals down to ultrasmall sizes, a structural change in the nanocrystal was suggested as the cause of the observed changes in the optical properties.[17]

While the emission at 440 nm involves a surface state, the emission at 488 nm is only slightly affected by the ligand exchange. Small amounts of alkylthiols have been shown to quench emission in CdSe nanocrystals, after the ligand exchange the feature at 488 nm is reduced in intensity, but is still present.[62] In the case of the dodecanethiol ligand exchange, the broad deep trap feature originally at 550 nm undergoes a significant redshift, due to the sulfur atom changing the surface energy.[63] The 488 nm feature is only observed in the emission spectrum after the onset of pinning (Fig. 3.3B). Since the ligand exchange will only affect the Cd atoms, the presence of the 488 nm feature after the ligand exchanges indicates that this feature may result from a surface state at Se atoms, as they were unaffected by the ligand exchange. The model of Puzder *et al.* predicts a mid-gap state that is located in the conduction band, further modeling places this mid-gap state on surface Se atoms after the nanocrystals have undergone a surface relaxation.

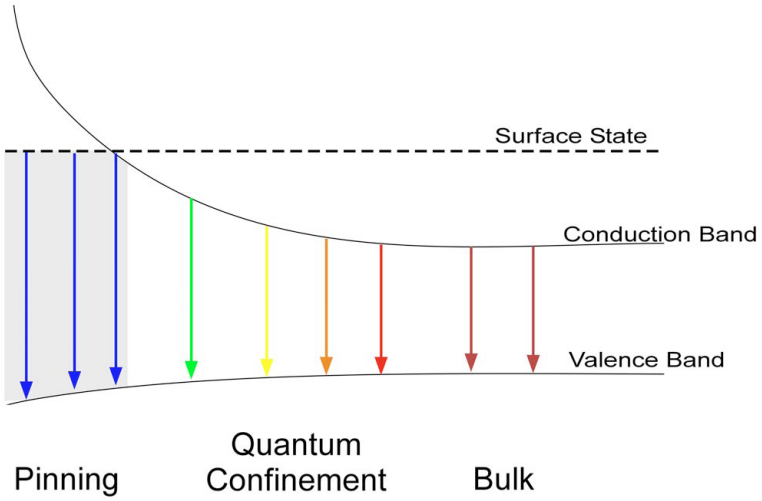

Figure 3.4: Model for pinned emission of the emission spectrum. At bulk sizes, CdSe has a fixed band gap energy. As CdSe enters the quantum confinement regime, the band gap becomes size dependent. However, at ultrasmall sizes, the emission spectrum becomes pinned (shaded box) when the conduction band becomes pinned (shaded box) when the conduction band becomes higher in energy than a size independent surface state.

Pinning can be explained as a result of emission from a surface state that has a fixed energy, which lies above the band gap of larger nanocrystals, but falls inside the band gap as the nanocrystal's diameter decreases below 2 nm and the band gap expands (Fig. 3.4). Thus, for small nanocrystals, the band-edge state is likely to be rapidly depopulated by a nonradiative transition that gives rise to the 440 nm emission peak. The assignment of a surface state is in agreement with Puzder *et al.*, whose theoretical work on ultrasmall CdSe indicated ~1 eV blueshift in the conduction band minimum relative to the bulk band gap.[56] As Fig. 3.2 shows, the first emission feature is fixed at 440 nm, or 2.8 eV, which is 1.06 eV blueshifted from the bulk band gap of CdSe (1.74 eV).[64] Puzder *et al.* attributed the blueshift to a surface state that occurred as a result of a surface relaxation; the nanocrystals would retain a wurtzite core, the surface would undergo significant rearrangement, altering the bond lengths by 25% and the bond angles by 25°.

While Lee *et al.* were unable to distinguish between surface and bulk states in their experiments, they did not rule out the possibility that surface states were responsible for the pinning.[57] In order to determine the exact nature of the surface state, ultrafast laser experiments are needed.

The emission spectrum for ultrasmall CdSe nanocrystals, passivated with alkyl phosphonic acids, with diameters of 1.7 nm and smaller, is shown to be pinned at 440 nm. While chain length is not observed to affect the wavelength of the pinned emission for the alkyl phosphonic acids used, the use of branched or unsaturated alkyl chains might alter the surface state sufficiently to pin the emission at a different wavelength. When the surface ligand is changed from a phosphonic acid to either dodecanethiol, oleic acid or pyridine, the emission at 440 nm is quenched. However, the positions of the remaining features are preserved, except in the case of the 550 nm emission for dodecanethiol. This indicates the pinning of the 440 nm emission peak is due to a surface state introduced by the phosphonic acid ligand binding to the surface of the nanocrystal.

3.4 Conclusions About Pinned Emission

Since the band edge absorption continued to blueshift with smaller sizes, this indicates that the pinning is not due to the Cd 5*s* /5*p* state being unaffected by quantum confinement. Instead, a surface state is responsible for the pinned emission because the absorption continues to blueshift while the emission spectrum is pinned at 440 nm. Additionally, a surface state related to Se atoms is proposed to be the cause of the emission at 488 nm. Since surface states are responsible for the unique emission properties in these ultrasmall CdSe nanocrystals, any device applications which utilize

the white emission spectrum of this material must preserve these states. This rules out traditional methods of enhancing their quantum yield, *i.e.*, shelling with a wider band gap material, and indicates that further research into the nature of these surface states is necessary.

CHAPTER IV

SYNTHESIS OF MAGIC-SIZE CADMIUM SELENIDE AND CADMIUM TELURIDE NANOCRYSTALS WITH DIISOOCTYLPHOSPHINIC ACID

4.1 History of Magic-Sized Nanocrystals

Magic-sized nanocrystals are composed of a well-defined number of atoms and only exist at certain stable sizes.[7,23,65] This allows the synthesis of large quantities of nanocrystals, all with identical properties, which cannot be achieved in traditional nanocrystal synthesis. The unique stability of magic-sized nanocrystals also differentiates them from traditional nanocrystals. Traditional CdSe nanocrystals have either wurtzite or zinc blende structure, while the stability of magic-sized nanocrystals is thought to arise from a cluster-cage structure.[8] The cluster-cage structure has yet to be reported for bulk semiconductors. This unique structure has only been accessible by a bottom-up synthetic approach.

Based on the result of mass spectrometry experiments, powder x-ray diffraction measurements, and theoretical modeling, Kasuya *et al.* have proposed that this cluster-cage structure is composed of alternating four- and six-membered rings, which allows for only certain sizes of nanocrystals.[8] They were able to synthesize several different sizes of the cluster-cage structure by using a reverse micelle synthesis, corresponding to $(CdSe)_{13}$, $(CdSe)_{33}$, and $(CdSe)_{34}$. The $(CdSe)_{33}$ and $(CdSe)_{34}$ have band edge absorption at 414 nm.[8] No other sizes were synthesized since only these sizes result in a closed cage structure. The largest size synthesized by Kasuya *et al.* corresponds to an external cage of

$(CdSe)_{28}$ that is stabilized by an internal structure of $(CdSe)_6$. To grow the next larger allowed size, it is thought that a new layer must be grown around the existing cage. This process would be observable by the appearance of a new peak in the UV-visible absorption spectrum that is redshifted from the previous band edge absorption. Such a unique redshift has been observed.[7,9,22] It is this quantized growth of the absorption spectrum that is the hallmark of true magic-sized nanocrystals.

Kudera *et al.* previously demonstrated quantized growth of CdSe nanocrystals.[7] Their synthesis utilized nonanoic acid to decompose CdO into a reactive precursor in an amine solvent, with an injection of Se dissolved in trioctylphosphine to begin the nanocrystal synthesis. The nanocrystals in the reaction solution were allowed to grow at 80 °C for up to 2500 minutes. The specific sizes of nanocrystals obtained from the quantized growth were those with band edge absorption peaks at 384 nm, 406 nm, and 431 nm. Their magic-size CdSe nanocrystals had a Cd:Se ratio between 1.1-1.3:1.[7] The fluorescence spectrum of these nanocrystals was broad and featureless, the result of trap-state emission. Kudera *et al.* observed band-edge recombination only after passivating the surface with a ZnS shell. When growth of the 431 nm-absorbing nanocrystals was allowed to continue, the nanocrystals no longer displayed quantized growth, but rather a continuous redshift in the absorption spectrum.

A recent study by Zanella *et al.* has investigated the optical properties of magic-sized II-VI nanocrystals.[22] Magic-sized nanocrystals were prepared by decomposing CdO with a carboxylic acid in the presence of a primary amine, followed by an injection of the anion (S, Se, or Te) dissolved in phosphines. The magic-sized CdTe nanocrystals with band-edge absorption at 445 nm (2.4 nm diameter, CdTe I) and band-edge absorption at

487 nm (3.1 nm is diameter, CdTe II) synthesized in their study displayed an intense, sharp emission spectrum. This was surprising, since the other II-VI nanocrystals of similar size had a broad emission spectrum dominated by trap states.[7,10,50] Zanella *et al.* also determined that the Cd:Te ratio for the magic-size nanocrystals was 1.2:1. This is the same cation:anion ratio that has been measured in traditional II-VI nanocrystals.[66]

In this study we demonstrate an alternative synthesis of magic-sized CdSe and CdTe nanocrystals and report on their optical properties. Magic-sized CdSe nanocrystals are synthesized with band-edge absorption peaks corresponding to 414 nm ($CdSe_{414nm}$), 446 nm ($CdSe_{446nm}$), and 490 nm ($CdSe_{490nm}$). The $CdSe_{414nm}$ synthesized in this study have a nearly identical absorption spectrum to the $(CdSe)_{33}$ and $(CdSe)_{34}$ synthesized by Kasuya *et al.*[8] Magic-sized CdTe nanocrystals with band edge absorption peaks of 445 nm ($CdTe_{445nm}$) and 483 nm ($CdTe_{483nm}$) were also synthesized. The $CdTe_{445nm}$ and $CdTe_{483nm}$ have a similar absorption spectrum to the CdTe I and CdTe II samples studied by Zanella *et al.*[22]

The magic-sized CdSe nanocrystals have a weak, broad-band fluorescence, while the magic-sized CdTe nanocrystals do not emit. Transmission electron micrographs did not provide a definitive crystal structure, but the images do show that the $CdSe_{414nm}$ magic-sized nanocrystals have a diameter of 1.7 nm and that $CdTe_{445nm}$ magic-sized nanocrystals have a diameter of 1.8 nm. The larger magic-sized $CdSe_{446nm}$ and $CdTe_{483nm}$ form ribbon structures with a diameter of 2.2 nm and 2 nm respectively. The synthesis described in this study allows for the isolation of larger sizes of magic-sized nanocrystals than have been previously reported. Additionally, we demonstrate that the interaction between the diisooctylphosphinic acid surface ligand and the coordinating solvent

hexadecylamine is responsible for the quantized growth of the magic-sized nanocrystals in this study.

4.2 Optical Properties

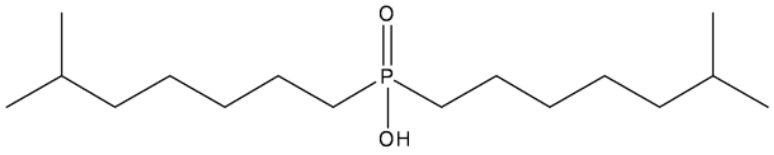

diisooctylphosphinic acid

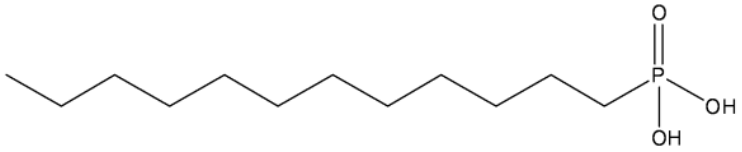

dodecylphosphonic acid

Figure 4.1: Structure of dodecylphosphonic acid and diisooctylphosphinic acid. Dodecylphosphonic acid, shown above, is a traditional ligand used to passivate the surface of CdSe nanocrystals. Diisooctylphosphinic acid is a liquid analog shown below. It is used to generate the reactive cadmium precursor and is used as the surface ligand for the CdSe and CdTe nanocrystals in this study.

Alkylphosphonic acids, such as dodecylphosphonic acid (Figure 4.1), have been employed in the synthesis of CdSe to achieve greater control over nanocrystal shape.[67] By varying the amount or type of phosphonic acid used in the synthesis, one can preferentially grow rods, dots, or tetrapods.[67,68] Nanocrystals that have been synthesized with alkylphosphonic acid surface ligands display a continuous redshift in their absorption spectrum as the nanocrystals grow to larger sizes.[45,50] Diisooctylphosphinic acid (Figure 4.1) is a liquid analog of an alkylphosphonic acid that is not widely used in II-VI nanocrystal synthesis. CdSe and CdTe nanocrystals were synthesized with diisooctylphosphinic acid as the surface ligand in an alkylamine coordinating solvent as

already described. When the reaction was arrested with the butanol injection, magic-sized CdSe nanocrystals, characterized by an extremely sharp (±0.16 nm particle diameter as determined from the absorption spectrum)[45] band edge absorption at 414 nm, were synthesized as shown in Figure 4.2A (no post-injection heating).[7,8] The magic-sized $CdSe_{414nm}$ nanocrystals have an additional feature in the absorption spectrum located at 383 nm, which is not usually observed in CdSe nanocrystals of this size.[10,18,50] It is possible that the 383 nm peak represents a smaller magic-size CdSe nanocrystal. While we were unable to isolate the 383 nm peak by itself, the location of this peak matches well with a previous report of magic-sized CdSe nanocrystals by Zanella *et al.* which have a band-edge absorption at 384 nm.[22]

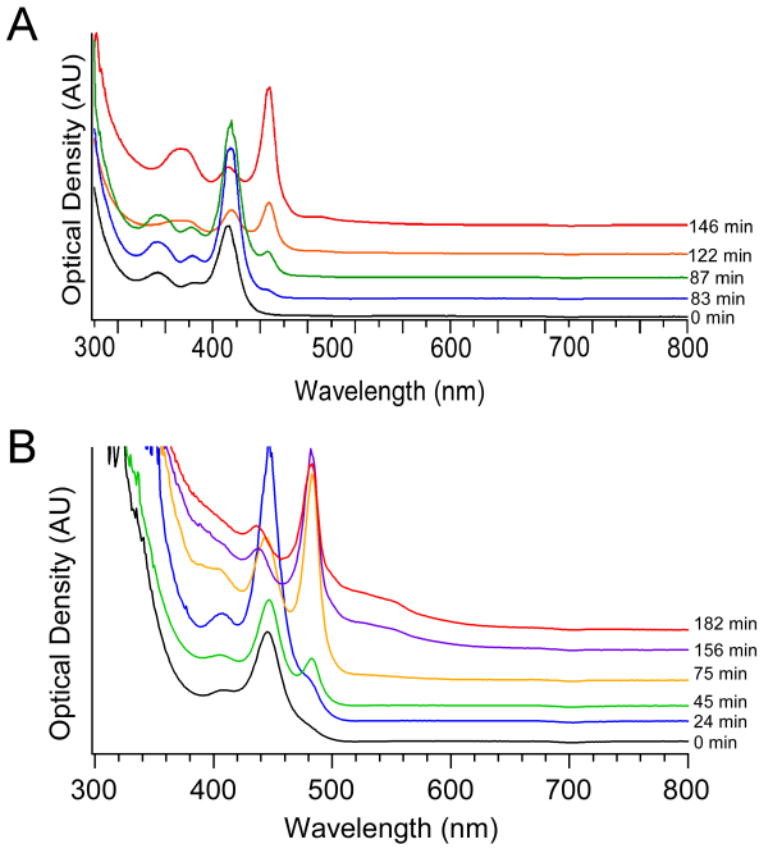

Figure 4.2: Absorption spectra of magic-size CdSe and CdTe nanocrystals. (A) The absorption spectrum of magic-sized CdSe nanocrystals, which have quantized growth, is shown above with the growth time for each measurement shown. Magic-sizes were observed corresponding to band edge absorption peaks at 414 nm, 446 nm, and 490 nm. (B) The absorption spectrum of magic-sized CdTe nanocrystals, which have quantized growth, is shown above with growth time for each measurement shown. Magic-sizes were observed corresponding to band edge absorption peaks at 445 nm and 483 nm. The peak observed to grow in at 540 nm marks the beginning of a continuous redshift, and is not a magic-size.

When the reaction flask was reheated to grow larger nanocrystals, the diisooctylphosphinic acid-capped magic-sized CdSe nanocrystals did not continuously grow. Instead, the diisooctylphosphinic acid-capped nanocrystals displayed a discontinuous redshift in their absorption spectra. This is characteristic of magic-sized nanocrystals.[9] As the magic-sized CdSe nanocrystals were heated, the band-edge absorption peak was observed to increase in intensity at 414 nm (Figure 4.2A). After 83

minutes of heating the magic-sized $CdSe_{414nm}$ nanocrystals, a new peak in the absorption spectrum was observed at 446 nm, while the peak at 414 nm persisted. As growth continued, the 446 nm peak increased in intensity without redshifting. After 146 min of growth a low intensity peak was observed at 490 nm. The peak intensity and position of the 490 nm peak remained unchanged even after heating overnight. The lack of growth to larger sizes is probably the result of insufficient precursors remaining in the reaction solution.

CdTe nanocrystals were also observed to undergo quantized growth with diisooctylphosphinic acid as the surface ligand. When the reaction was quenched, as shown in Figure 4.2B (no post-injection heating), a sharp peak in the absorption spectrum was observed at 445 nm, characteristic of magic-sized CdTe nanocrystals.[9,22] After 24 minutes of growth, a peak at 483 nm was observed to grow in while the peak at 445 nm remained. The peak at 483 nm continued to increase in intensity over time. The next peak to appear in the absorption spectrum was very weak and centered around 540 nm. This peak began to continually redshift with heating. Thus these could not be considered to be magic-sized CdTe nanocrystals. Two distinct sizes of magic-sized CdTe nanocrystals were grown, corresponding to band-edge absorption peaks at 445 nm and 483 nm.

Our smallest magic-sized CdSe nanocrystal, $CdSe_{414nm}$ has a similar band edge absorption to the 406 nm previously observed by Kudera *et al.*[7] CdSe nanocrystals with band edge absorption at 446 nm were reported to be in the continuous growth size regime in Kudera's study. However, the results presented in this study indicate that it is possible to have stable magic-sized nanocrystals with band edge absorption at 446 nm (Figure 4.2A). The main difference between the nanocrystals synthesized in this study and those

synthesized by Kudera is the surface-passivating ligand. Where Kudera used nonanoic acid, this study utilized diisooctylphosphinic acid as the surface ligand. The diisooctylphosphinic acid ligand binds tighter to the nanocrystal surface[69] and allows for the growth of larger magic-sized CdSe nanocrystals.

The smallest magic-sized CdTe nanocrystals, $CdTe_{445nm}$, synthesized in this study match those of Zanella *et al.* with a band edge absorption peak at 445 nm.[22] We observed larger magic-sized CdTe nanocrystals similar to the CdTe II reported by Zanella (band edge absorption of 483 nm compared to 487 nm). The difference arises in the fact that the magic-sized CdTe nanocrystals synthesized in this study have an increased selectivity over previous work. Zanella was unable to grow the 487 nm-absorbing magic-size (CdTe II), without also growing the 506 nm-absorbing magic-size (CdTe III) simultaneously. By choosing diisooctylphosphinic acid it was possible to grow $CdTe_{483nm}$ nanocrystals in the absence of any larger sizes.

The magic-sized CdTe synthesized by Zanella *et al.* had an intense and narrow emission spectrum.[22] The CdTe nanocrystals synthesized in this study do not emit. The emission spectrum of $CdSe_{414nm}$, shown in Figure 4.3A has a similar broad-band emission that has been previously observed in ultrasmall CdSe nanocrystals capped with dodecylphosphonic acid.[10,18,50,70] The broad emission is spread over most of the visible spectrum and has a quantum yield of 0.8 %. The measured quantum yield is an order of magnitude lower than the 8 % quantum yield of white-light emitting CdSe nanocrystals that are of similar size and capped with dodecylphosphonic acid.[71] The $CdSe_{446nm}$ still have significant trap state emission (Figure 4.3B).

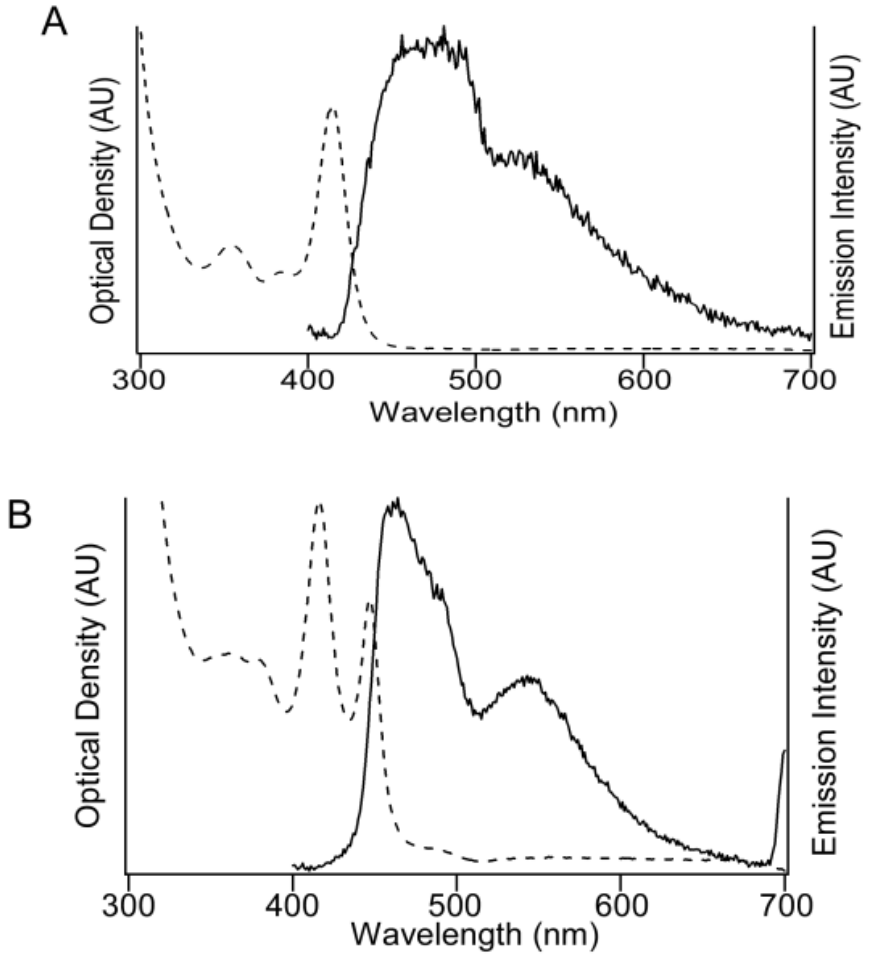

Figure 4.3: Absorption and emission spectra of $CdSe_{414nm}$ and $CdSe_{446nm}$ magic-size nanocrystals. The absorption (dashed lines) and emission (solid lines) are shown for (A) $CdSe_{414nm}$, and (B) $CdSe_{446nm}$. The $CdSe_{414nm}$ nanocrystals have a broad emission similar to that of the alkylphosphonic acid capped nanocrystals.[10] Growth to the next larger sizes results in a narrowed emission spectrum with the persistence of deep-trap emission.

Photoluminescence excitation (PLE) measurements were performed on the magic-sized CdSe nanocrystals to determine the reason for the low quantum efficiency observed. As shown in Figure 4.4, absorption events at the band edge of the magic-sized CdSe nanocrystals do not lead to radiative recombination. Previous studies of the excitation spectrum of CdSe nanocrystals have shown that absorption at the band edge leads to the most efficient radiative recombination.[72] The weak emission that was

observed is likely due to trap-state emission occurring at surface defects. Further, the PLE spectra show that these trap states, which relax radiativly, are populated as a result of absorption events in the continuum. Previous studies have shown that an electron from a surface Se atom can relax to fill the vacancy left in the valence band by the photo-generated electron, resulting in trap state emission.[73,74]

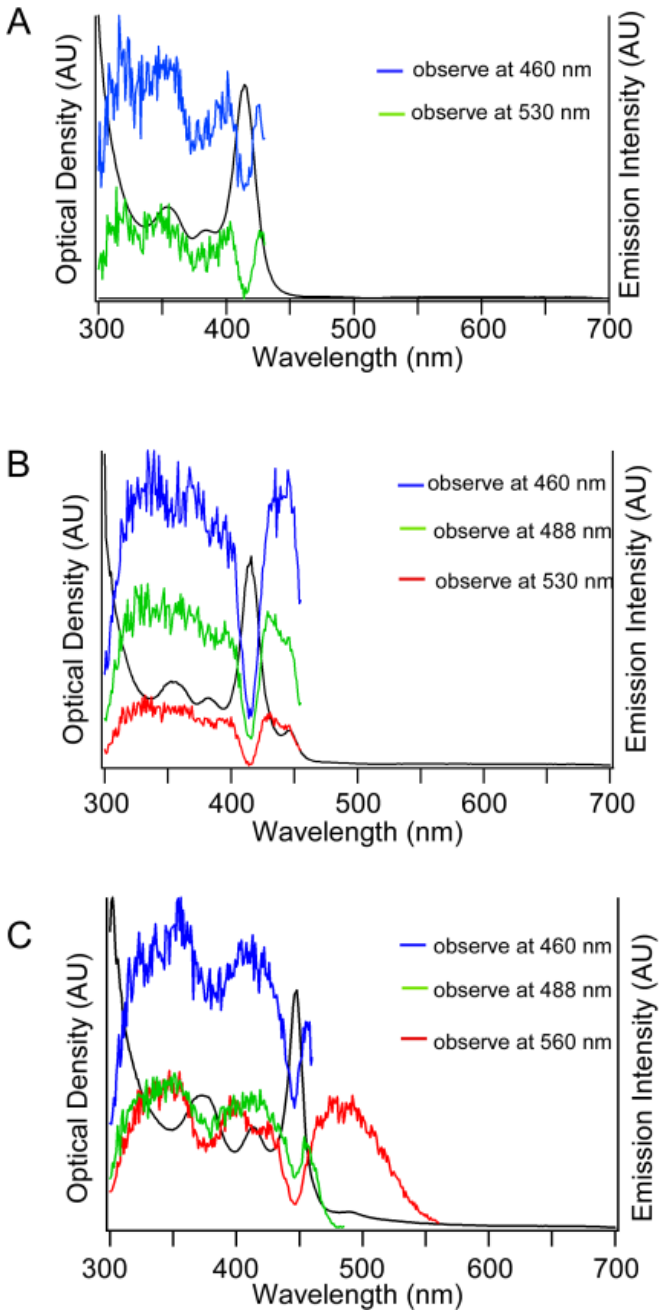

Figure 4.4: Photoluminescence excitation spectra of magic-size CdSe nanocrystals. The photoluminescence excitation scans (colored lines) reveal the absorbing states that are responsible for each emission peak. The absorption spectrum of each sample is shown in the black curves. PLE scans for A: $CdSe_{414nm}$ nanocrystals, B: Mixture of $CdSe_{414nm}$ and $CdSe_{446nm}$ nanocrystals, C: $CdSe_{446nm}$ nanocrystals. In each sample, the PLE scans showed significantly reduced emission intensity for the absorption peaks corresponding to band edge absorption.

There are three possible reasons why the magic-sized diisooctylphosphinic acid-capped nanocrystals do not emit via band edge absorption. The first possibility is that they have a unique crystal structure that could alter their optical properties. The second possibility is that the steric effects of the secondary phosphinic acid lower the quantum yield. The third possibility is that the magic-sized CdSe nanocrystals have an internal atomic defect (an extra atom or a missing atom) that creates a non-radiative trap state. A sample of dodecylphosphonic acid capped CdSe nanocrystals were synthesized and used in a ligand exchange as already described. The initial quantum yield of the CdSe nanocrystals was 6.4 %. After the ligand exchange to diisooctylphosphinic acid, the CdSe nanocrystals had a quantum yield of 0.3 %. The almost complete quenching of the emission in the nanocrystals is therefore likely the result of the steric effect of the secondary phosphonic acid replacing the alkylphosphonic acid.[63] The secondary ligand would be expected to leave some surface sites unpassivated,[63] resulting in the weak trap state emission observed in the $CdSe_{414nm}$ nanocrystals.

4.2.1 Synthetic Conditions for Magic-Sized Nanocrystals

Reaction Conditions	**Observation of Quantized Growth**
10 g 99% TOPO	Not Observed
10 g 90% TOPO	Not Observed
10 mL 1-Octadecene	Not Observed
5:1 Cd:Se molar ratio in 10g HDA	Not Observed
10 g HDA and 2 mmol Dodecylphosphonic acid	Continuous Growth
1:5 Cd:Se molar ratio in HDA	Quantized Growth Observed
5 g TOPO (90%) 5g HDA	Quantized & Continuous Growth Observed

Table 4.1: Synthetic conditions used to synthesize magic-size nanocrystals**.** A summary of the solvent and reaction conditions with diisooctylphosphinic acid is shown. All reactions are carried out with a 2:1 molar ratio of diisooctylphosphinic acid to CdO unless otherwise noted.

The synthesis of the magic-sized CdSe nanocrystals was repeated using various solvents to determine if the quantized growth resulted solely from the diisooctylphosphinic acid, or if the coordinating solvent also affected the growth. In all of the reactions summarized in Table 4.1, the 2:1 molar ratio of diisooctylphosphinic acid to CdO was maintained, and the 1:1 molar ratio of Cd:Se was maintained unless otherwise noted.

When the reaction was conducted in tri-n-octylphosphine oxide (TOPO), quantized growth in the absorption spectrum was not observed. When the reaction was performed with 1-octadecene as the non-coordinating solvent, quantized growth of the absorption spectrum was also not observed (Fig. 4.5).

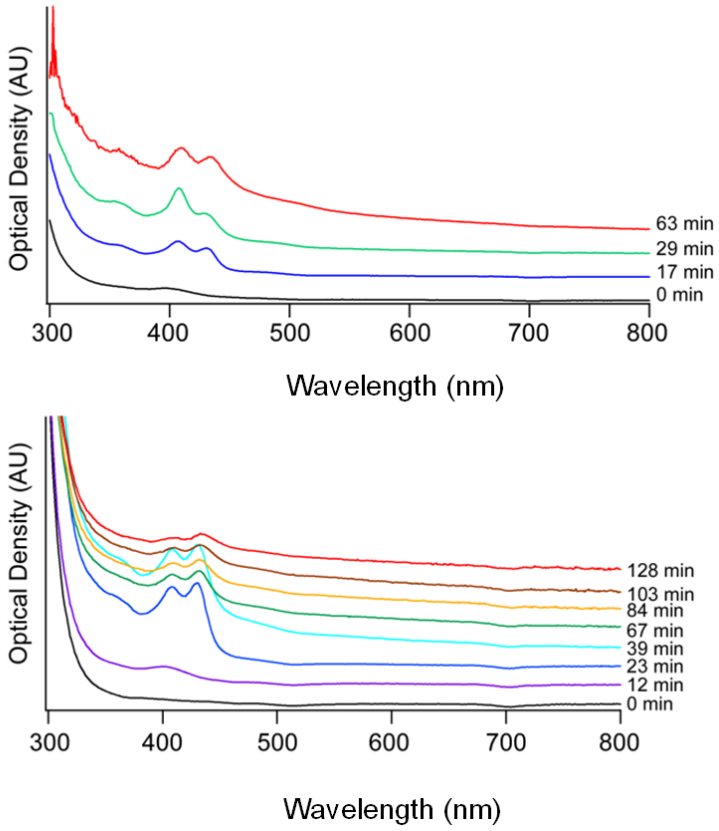

Figure 4.5: Absorption spectra of magic-sized nanocrystals with TOPO and ODE as the solvent. The absorption spectrum of CdSe capped with diisooctylphosphinic acid synthesized in TOPO (top) and ODE (bottom). Quantized growth is not observed when these solvents are used.

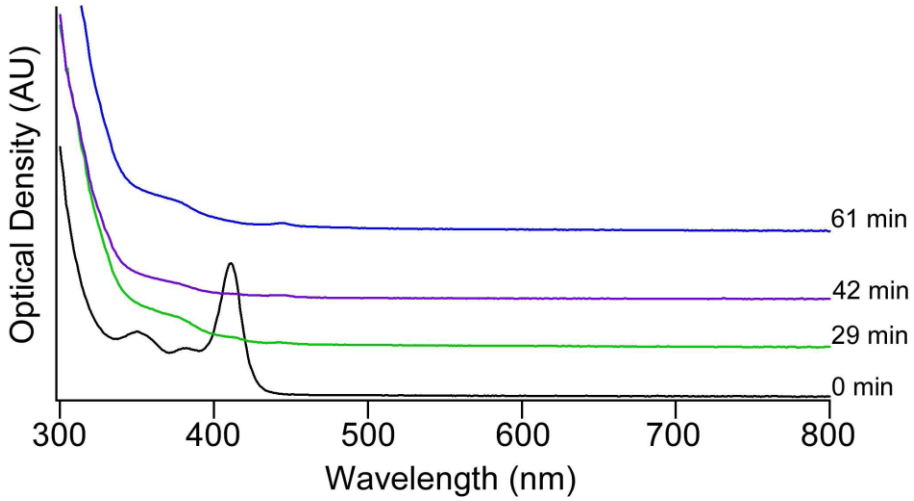

Figure 4.6: Absorption spectra of magic-size nanocrystals under Cd-rich conditions. The absorption spectrum with growth times of CdSe nanocrystals synthesized with diisooctylphosphinic acid in HDA with a Cd:Se ratio of 5:1.

The initial absorption spectrum from the Cd-rich synthesis matches that of magic-sized CdSe nanocrytals (Figure 4.6, 0 min of post injection heating). However, when these nanocrystals were heated, the absorption spectrum showed that the band edge absorption at 414 nm had disappeared. This is likely the result of excess diisooctylphosphinic acid etching the nanocrystals during growth. While the same amount of diisooctylphosphinic acid was used in this synthesis, lowering the amount of Se injected led to fewer nanocrystals being formed, which resulted in a larger concentration of acid than normal. The higher acid concentration was sufficient to almost completely etch away the nanocrystals in 29 minutes.

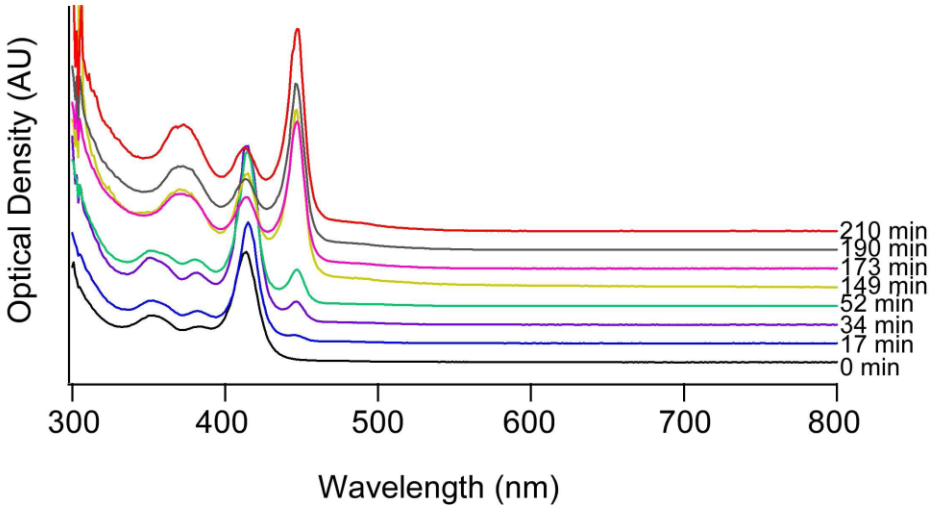

Figure 4.7: Absorption spectrum of magic-sized nanocrystals under Se rich conditions. The absorption spectrum with growth times of CdSe nanocrystals synthesized with diisooctylphosphinic acid in HDA with a Cd:Se ratio of 1:5.

When the reaction was performed under Se rich conditions quantized growth of magic-sized CdSe nancorystals was observed as shown in Figure 4.7. In order to reduce the impact of a large concentration of phosphines, a more concentrated Se solution was used, 1.5 M. After 34 minutes of growth, the absorption peak corresponding to the second magic-size was observed. After 149 minutes the peak at 490 nm was observed to grown in. No peaks were observed to be redshifted beyond 490 nm even after 210 minutes.

The synthesis was also carried out in a mixed solvent system of 5 g TOPO and 5 g HDA. When the reaction was arrested with the butanol injection, the absorption spectrum showed a peak at 414 nm that was identical to previous amine-only synthesis which yielded magic-sized CdSe nanocrystals. When the reaction solution was reheated to 150 ºC for growth, a new peak was observed in the absorption spectrum (Fig 4.8). With continued heating, this new peak was observed to continuously redshift. However, the

main peak at 414 nm remained and became more intense. This was indicative of two distinct populations of nanocrystals in the reaction solution.

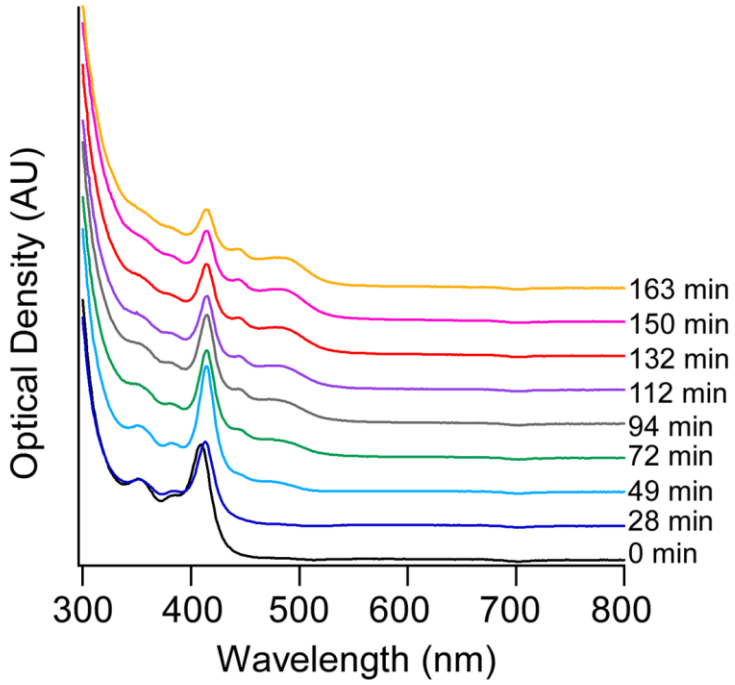

Figure 4.8: Absorption spectra of magic-sized nanocrystals in a TOPO/HDA mixed solvent system. The absorption spectrum of magic-sized CdSe nanocrystals grown in a mixed TOPO/HDA solvent system results in two populations of nanocrystals.

After 72 minutes of growth in the mixed TOPO/HDA solvent, a new peak was observed in the absorption spectrum at 446 nm (Figure 4.8). This is the same location that the $CdSe_{446nm}$ nanocrystals were previously observed. The largest magic-sized CdSe nanocrystals ($CdSe_{490nm}$) were not observed in the mixed solvent system. This was likely the result of the signal from the continuous growth population overwhelming the weak signal that was previously observed for this magic-size. The continuous growth observed in this reaction was due to the presence of TOPO in the solvent system, and the quantized growth was due to the combination of the hexadecylamine and the diisooctylphosphinic

acid. Previous studies on magic-sized CdTe and CdSe nanocrystals have involved a synthesis that employs an alkylamine as a coordinating solvent.[7,9,22] None of these previous studies reported on attempts to synthesize magic-sized II-VI nanocrystals without an alkylamine as the coordinating solvent. In this study, quantized growth is only observed when the alkylamine solvent is present with the diisooctylphosphinic acid. This indicates diisooctylphosphinic acid alone is not responsible for the quantized growth. Rather the surface-passivating ligand and the alkylamine act together producing the quantized growth in magic-sized nanocrystals. As a control nanocrystals were then synthesized with dodecylphosphonic acid and HDA (Fig 4.9) and continuous growth was observed.

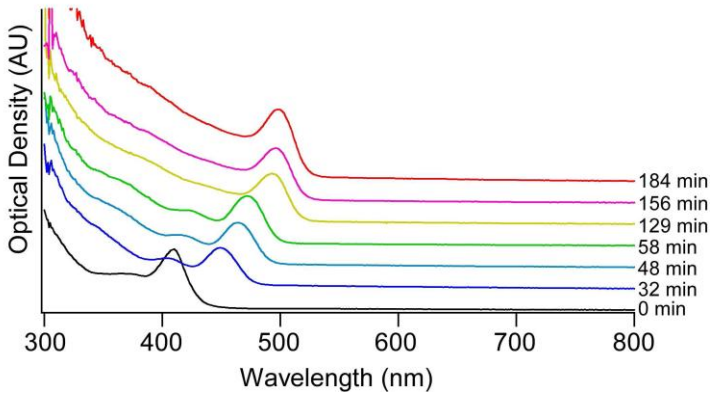

Figure 4.9: Absorption spectra of nanocrystals with dodecylphosphonic acid. The absorption spectrum with growth times of CdSe nanocrystals synthesized with dodecylphosphonic acid in 10 g of HDA is shown.

The previously published cluster-cage model for magic-sized CdSe nanocrystals may explain the quantized growth observed in our nanocrystals.[8] The cluster-cage model proposes a structure that is composed of only mixed surfaces, unlike the wurtzite structure that has both polar and mixed surfaces. Surface ligands have been shown to

inhibit crystal growth on the more thermodynamically stable mixed surfaces.[69] Additionally, phosphinic acids and amines bind tighter to the mixed surface than other surface ligands such as phosphine oxides.[69] When TOPO was used as a coordinating solvent, continuous growth was not observed (Figure 4.5) because the mixed surface is more available to react with the Cd and Se in the reaction solution. The phosphinic acid ligand also binds to the mixed surface in the same location as a CdSe molecule would bind.[69] If the surface ligand is occupying the same site that the Cd or Se need to access in order to bind, then growth of successive layers will be severely inhibited. Theoretical calculations have shown that branched ligands, like diisooctylphosphinic acid, will bind less tightly to the nanocrystal surface than primary ligands of the same functionality because of steric hindrance.[75] This reduction in binding energy due to steric effects is likely to be sufficient to allow the Cd and Se to displace some surface ligands resulting in the slow nanocrystal growth observed. Modeling of the cluster-cage structure by Kasuya *et al.* has shown that cage configurations are more stable with a certain number of atoms, which maximizes the Cd to Se binding energy in the nanocrystal.[8] It is likely that the addition of several Cd and Se atoms during a short time is necessary to achieve a larger, stable structure. The addition of several atoms at once would manifest as a discrete red-shift in the absorption spectrum. This is similar to the quantized growth we and others have observed. This result confirms previous findings that a strongly binding surface ligand and coordinating solvent are necessary for the growth of magic-sized nanocrystals.[9]

4.3 Structural Properties of Magic-Sized CdSe and CdTe Nanocrystals

The $CdSe_{414nm}$ nanocrystals have an absorption spectrum that is remarkably similar to the 414 nm absorbing nanocrystals previously synthesized by Kasuya *et al*.[8] The absorption spectrum of Kasuya's nanocrystals is interesting because it has a higher energy transition that is not observed in CdSe nanocrystals synthesized with an alkyl phosphonic acid.[10,50] The $CdSe_{414nm}$ synthesized in this study have the same high energy transitions observed by Kasuya *et al.*, which leads to the conclusion that they probably possess the same structure. X-ray diffraction measurements were performed on the magic-sized nanocrystals with no peaks observed, which is likely due to the small diameter of the nanocrystals.

Magic-sized $CdSe_{446nm}$ nanocrystals were dispersed on few-layer graphene, which was synthesized using previously published methods.[76] Using graphene as the support layer for imaging CdSe and CdTe nanocrystals significantly reduces the background signal compared to the traditional carbon supports.[76] The samples were imaged immediately after the cleaning procedure because the magic-sized nanocrystals photo-oxidize after several hours, resulting in sample degradation. The images show that the $CdSe_{446nm}$ arrange together to form long ribbon structures (Figure 4.10 A and B). The ribbons have a diameter of 2.2 nm, which is in good agreement with the sizing equations developed by Yu *et al.* which predicts a diameter of 2.19 nm.[45] The smaller $CdSe_{414nm}$ magic-sized nanocrystals were also imaged on few-layer graphene and are shown in Figure 4.10 C and D. At the smallest sizes, the magic-sized CdSe nanocrystals appear spherical. The magic-sized $CdSe_{414nm}$ nanocrystals have a diameter of 1.7 nm which is

again in good agreement with the sizing equations of Yu *et al.* which predicts a diameter of 1.67 nm.

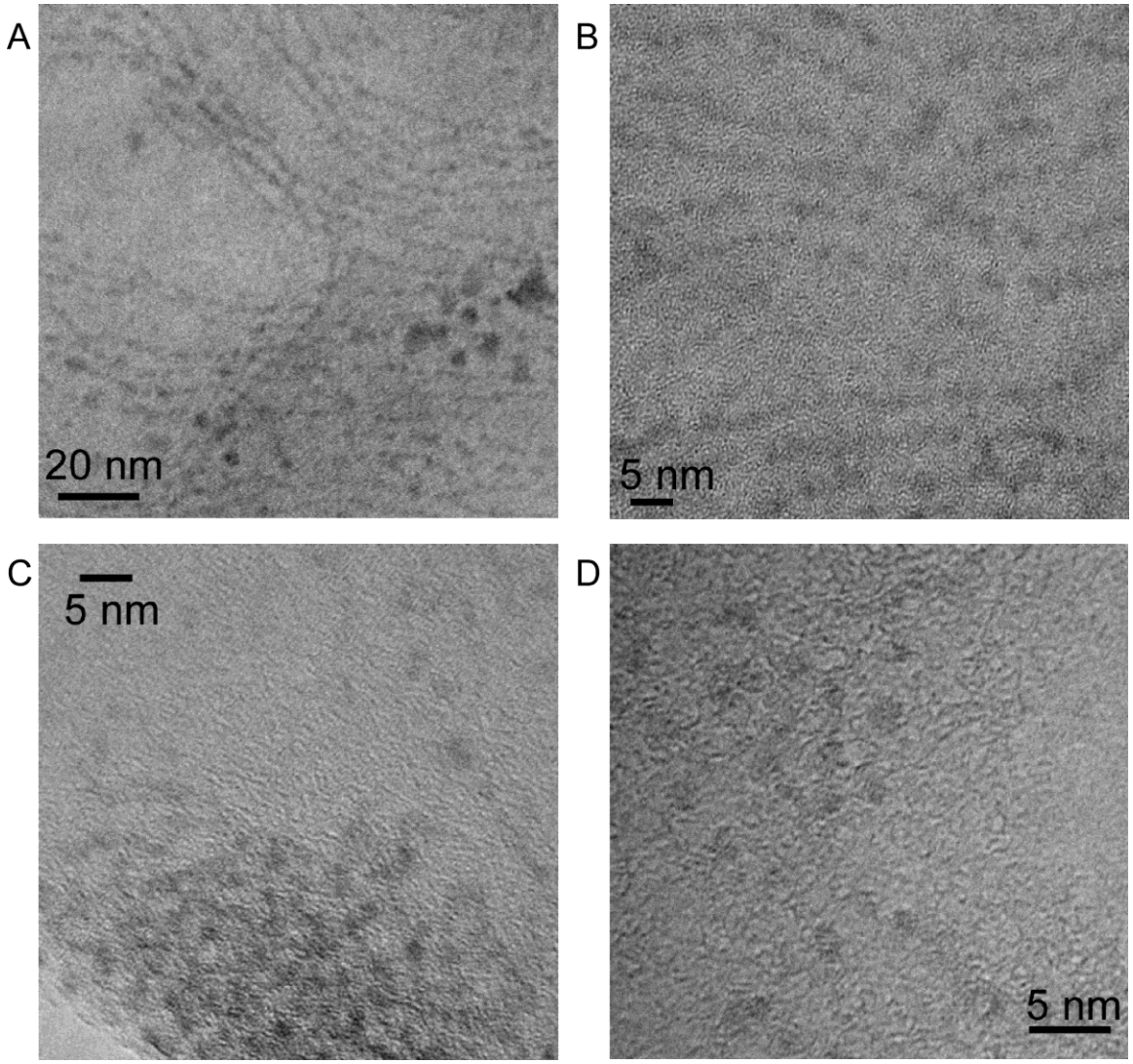

Figure 4.10: TEM micrographs of $CdSe_{414nm}$ and $CdSe_{446nm}$ magic-sized nanocrystals. TEM images of $CdSe_{446nm}$ magic-sized nanocrystals are shown in panels A and B. TEM images of $CdSe_{414nm}$ are shown in panels C and D. All magic-sized nanocrystals were imaged on few-layer graphene.

A morphological change is apparent between the $CdSe_{446nm}$ nanocrystals shown in Figure 4.10 A and B and the$CdSe_{414nm}$ shown in Figure 4.10 C and D. The ribbon

structures observed for the $CdSe_{446nm}$ nanocrystals are similar to previously observed nanoribbons.[44,77,78] Further, the absorption spectrum of the $CdSe_{446nm}$ as shown in Figure 3B is consistent with the values of previous reports for nanoribbions. Previous work by Joo *et al.* reported absorption peaks at 449 nm and 423 nm, while Liu *et al.* reported absorption peaks at 447 nm and 420 nm.[44,78] It appears that the $CdSe_{414nm}$ magic-sized nanocrystals form nanoribbon structures as they grow into the $CdSe_{446nm}$ magic-sized nanocrystals. As the $CdSe_{446nm}$ magic-sized nanocrystals continue to grow their absorption spectrum deviates from the previously published absorption spectrum of nanoribbons.[44,78] It is possible that this represents another morphological change in the magic-sized CdSe nanocrystals; however, no change was observed in the TEM.

Magic-sized $CdTe_{483nm}$ nanocrystals were dispersed on few-layer graphene. The larger magic-size of CdTe nanocrystals also forms ribbon structures (Figure 4.11 A and B) with a similar appearance to the ribbon structures formed by $CdSe_{445nm}$. The $CdTe_{483nm}$ has a diameter of 2 nm. A diameter for the CdTe magic-sized nanocrystals was not able to be estimated from the sizing equations of Yu *et al.* $CdTe_{445nm}$, shown in Figure 4.11 C and D, have a diameter of 1.8 nm. Some larger nanocrystals were present in the CdTe samples. They may be the result of nanocrystals aggregating as the solvent evaporates from the TEM grid since there was no peak corresponding to these aggregates in the absorption spectrum.

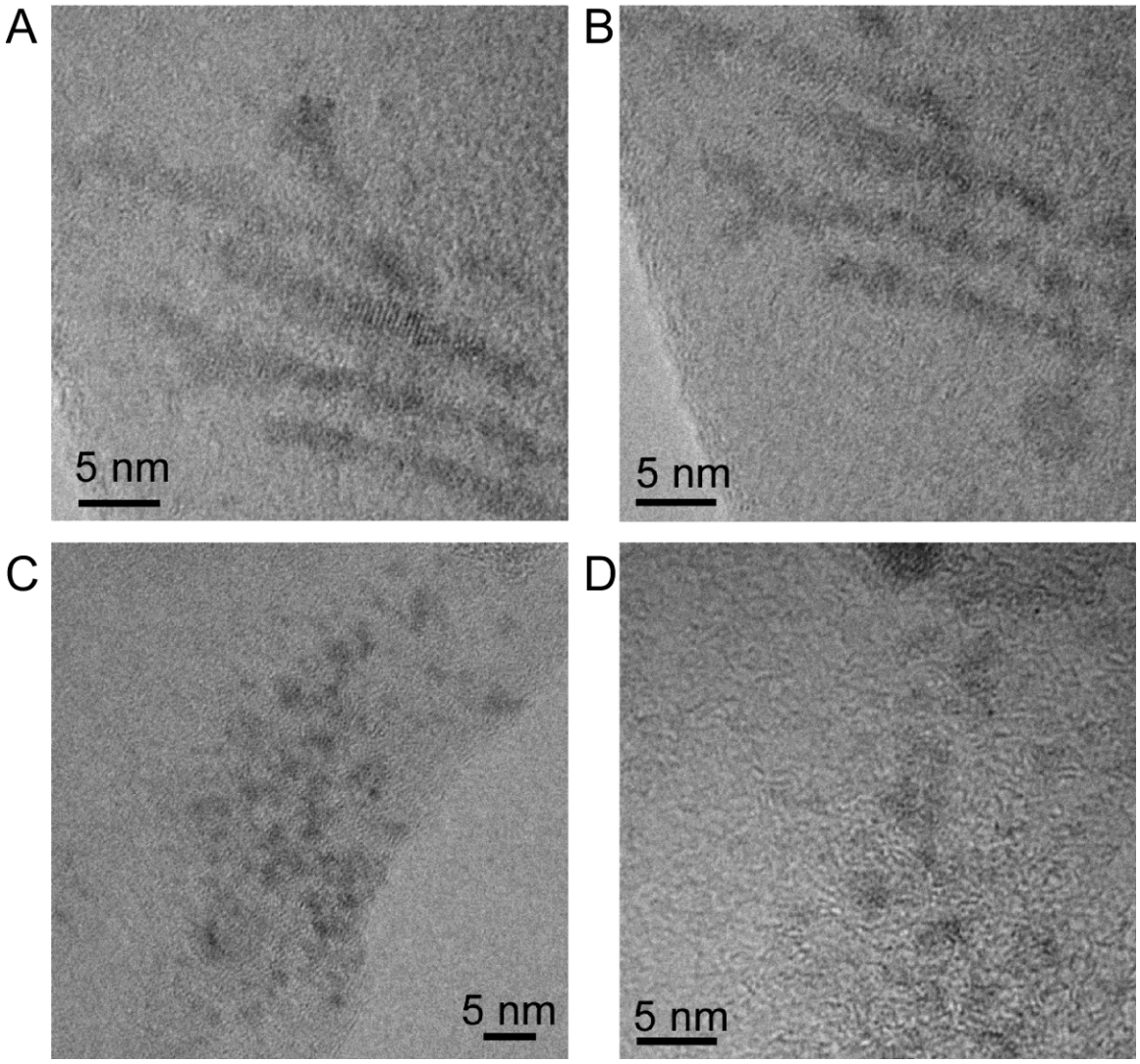

Figure 4.11: TEM micrographs of $CdTe_{483nm}$ and $CdTe_{445nm}$ magic-sized nanocrystals. TEM images of $CdTe_{483nm}$ magic-sized nanocrystals are shown in panels A and B. TEM images of $CdTe_{445nm}$ are shown in panels C and D. All magic-sized nanocrystals were imaged on few-layer graphene.

While the magic-sized nanocrystals that are reported here are the correct size, we cannot conclusively determine if they match the cluster-cage structure predicted by Kasuya *et al.* Lattice resolved images on CdSe nanocrystals have been obtained previously on nanocrystals of similar diameter, which were synthesized using an

alkylphosphonic acid as the surface ligand.[76] While the lack of lattice resolution in these images appears consistent with the cluster-cage model proposed by Kasuya; because alternating four- and six- member rings in a 3D structure would not be expected to produce the regular columns of atoms needed for a lattice resolved image. It is possible that the clean-up procedure utilized in this study did not completely remove excess surfactants. The methanol-hexanol-methanol wash cycle employed to clean up the ultrasmall CdSe nanocrystals by McBride *et al.*[76] resulted in the degradation of the absorption spectrum when used on magic-sized CdSe and CdTe nanocrystals in this study. The presence of excess surfactants could result in lower-resolution images than previously observed in cleaner samples.

A recent study by Nguyen *et al.* calculated several different possible structures for magic-sized CdSe nanocrystals.[79] The $CdSe_{445nm}$ nanocrystals synthesized in this study have the same band edge absorption (2.78 eV) to the $(CdSe)_{30}$ tube with S_6 geometry proposed by Nguyen (2.78 eV).[79] The predicted diameter of 2.06 nm for $(CdSe)_{30}$ differs from the measured diameter for $CdSe_{445nm}$. The calculated $(CdSe)_{24}$ tube diameter of 1.65 nm is a closer match to $CdSe_{414nm}$. However, the energy of the band edge transition (2.83 eV) does not match well with $CdSe_{414nm}$.[79] A possible source of the differences could be the ligand passivation. The study by Nguyen *et al*. used an amine as the surface ligand where we have utilized a phosphinic acid.

4.4 Conclusion about Magic-Sized CdSe and CdTe Nanocrystals

Magic-sized CdSe and CdTe nanocrystals were synthesized with diisooctylphosphinic acid as the surface ligand. The magic-sized nanocrystals have a

quantized growth mechanism that only allows for distinct sizes of nanocrystals to be synthesized. The observed trap-state recombination in the fluorescence spectrum is the result of absorption from the continuum states above the band-edge. The steric effects of the secondary phosphinic acid ligand result in very little emission from band edge absorption. TEM measurements showed that the magic-sized $CdSe_{414nm}$ nanocrystals have a diameter of 1.7 nm, and the magic-sized $CdTe_{445nm}$ nanocrystals have a diameter of 1.8 nm. The magic-sized nanocrystals also undergo a morphological change and are shown to form nanoribbons at larger sizes. The synthesis described here results in larger magic-sized nanocrystals than have been previously reported. The work also emphasizes the critical role that surface ligands play in the formation of nanostructures. The synthesis of larger magic-sizes provides an opportunity for detailed structural study utilizing scanning transmission electron microscopy (STEM). The superior resolution provided by STEM has been used to study nanocrystals of similar size previously,[18] and could provide insight to the origin of the stability of magic-size nanocrystals.

CHAPTER V

SINGLE-NANOCRYSTAL SPECTROSCOPY OF WHITE-LIGHT EMITTING CADMIUM SELENIDE NANOCRYSTALS

5.1 Previously Observed Optical Properties of White-Light CdSe Nanocrystals

Ultrasmall nanocrystals, those with a diameter of less than 2 nm, have recently become an active research area as they have properties that differ markedly from larger nanocrystals.[5,7,10,11,18,22,25,26,50,70,80,81] These properties include quantized growth,[7,22] a size-independent emission spectrum,[50,70] and white light-emission.[10,11,18,25,26,80,81] Of these unique properties, white-light emission in CdSe nanocrystals has stimulated particular interest because of its potential for application in light-emitting diodes and solid state lighting applications requiring excellent color rendering.[26]

Ultrasmall CdSe nanocrystals have an almost pure white-light emission spectrum with chromaticity coordinates of (0.322, 0.365) on the 1931 CIE diagram.[10] As shown in Figure 5.1, white-light emitting CdSe nanocrystals have a sharp band-edge absorption, indicating that the sample is monodisperse. The broad emission spectrum shown in Figure 5.1 is not typical of a monodisperse population of nanocrystals. While deep-trap emission has been observed as a broad peak significantly redshifted from the band edge, the three distinct peaks observed in the emission spectrum in Figure 1 are not observed in larger nanocrystals.

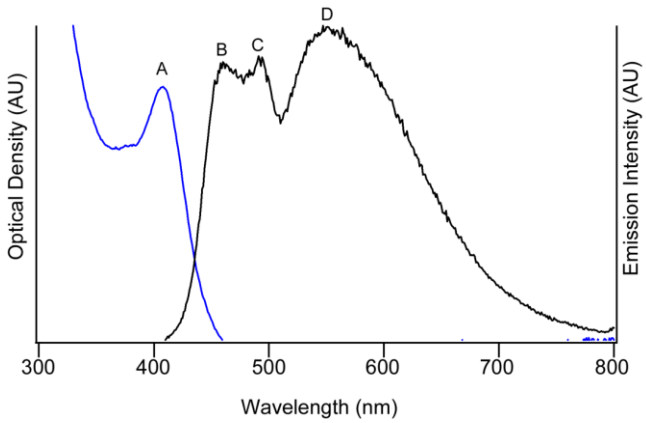

Figure 5.1: Ensemble absorption and fluorescence spectrum of white-light emitting CdSe nanocrystals. The ensemble absorption (blue curve) and fluorescence spectra (black curve) for the white-light emitting CdSe nanocrystals are shown. The band-edge absorption peak is 408 nm (A). The narrow peak and sharp band-edge in the absorption spectrum indicate that the nanocrystal sample is monodisperse. The white-light fluorescence spans the majority of the visible spectrum with peaks at 450 nm (B), 490 nm (C) and 550 nm (D), resulting in a white-light emission spectrum.

There are two possible explanations for the white-light emission observed in the ensemble spectrum shown in Figure 5.1. The first is that each CdSe nanocrystal has several different trap states on its surface required for white-light emission. The second scenario is that there are at least three energetically different trap states distributed among the entire population, with each nanocrystal having distinct traps. This would result in the observation of each nanocrystal emitting only a narrow portion of the spectrum. In order to determine which explanation holds, we have designed and constructed a single-nanocrystal spectroscopy instrument.

Early work on the emission of white-light CdSe nanocrystals has determined that the emission spectrum is size-independent, or pinned.[50] It was observed that the first emission feature ceased to blueshift once the band edge absorption reached 420 nm, though the band edge absorption continued to blueshift with decreasing nanocrystal diameter.[50,70] This indicates that while the blue emission peak appears to be band-edge

recombination, the peak is actually the result of trap-state recombination.[50] Further work has demonstrated that the trap state involves the surface passivating ligand, and that changing the ligand can change the wavelength of the blue emission peak.[50,70]

Surface ligands are not the only way to modulate the white-light emission spectrum from CdSe nanocrystals.[81] Quain *et al.* demonstrated that by allowing the reaction to proceed for longer periods of time, the emission color could be tuned from a warm white to a cool white.[81] This was accomplished by slightly varying the time that the nanocrystals were allowed to grow. As the nanocrystals grew to larger sizes, the trap states responsible for the broad emission were eliminated. Additionally, nanocrystal growth resulted in a more pronounced blue emission peak. While white-light electroluminescence has been demonstrated,[26] the work of Quain *et al.* indicates that it should be possible to tailor the emission of white-light-emitting diodes employing nanocrystals to consumer preference.

The emission properties of white-light emitting CdSe nanocrystals were also investigated by Bowers *et al.,* who utilized ultrafast fluorescence upconversion spectroscopy to determine the origin of the broad emission in this material.[18] They conducted measurements at five wavelengths in the emission spectrum (459 nm, 488 nm, 535 nm, 552 nm, and 585 nm), while exciting the nanocrystals at 400 nm for each measurement. They observed that the radiative lifetime increased as the spectrum evolved from blue to red, similar to a fluorescent molecule. Bowers *et al.* concluded that much of the broad emission was the result of trap-state recombination. The shorter lifetimes were attributed to the extreme confinement of the white-light emitting nanocrystals due to their diameter of 15 Å.[18] In addition to the fluorescence

upconversion studies, Bowers *et al.* imaged the white-light emitting CdSe nanocrystals using aberration corrected scanning transmission electron microscopy. These images showed that the nanocrystals have defects in their crystalline structure, missing or extra atoms, which could create trap states.[18]

While the work performed by Bowers *et al.* established that the broad emission was the result of trap-state recombination, their technique was unable to interrogate individual nanocrystals and was reliant only on ensemble measurements. Left unanswered was the question of whether each nanocrystal emits all three peaks, or if there is a distribution of distinct subgroups within the ensemble that are effectively monochromatic. If an individual nanocrystal emits only a portion of the ensemble spectrum, it is possible that this is the result of structural variations of the nanocrystals within the sample. However, if each nanocrystal emits the entire broad spectrum, it is likely that each nanocrystal has essentially the same structure.

In this study, we report the observation of broad spectrum, white-light emission from individual CdSe nanocrystals. The white-light emitting CdSe nanocrystals are observed to blink, which is the classic signature of individual nanocrystal emission. Further, the light from the blinking nanocrystals is white and uniform. These results indicate that each white-light emitting nanocrystal contains all the trap states needed for the white-light emission observed in the ensemble spectrum.

5.2 Description of Single-Nanocrystal Fluorescence Spectrometer

A schematic of the single-nanocrystal spectroscopy experiment is shown in Figure 2. The sample is excited with wide-field epi-illumination using the 400 nm beam from a frequency-doubled Ti-Sapphire laser. This is produced by using a 1 mm thick β-BBO crystal (Altos Photonics) for Type I angle-tuned frequency doubling of the 800 nm beam from a 76 MHz femtosecond Ti-Sapphire oscillator (Coherent Mira 900 Basic). The residual 800 nm light is removed by a 425 nm bandpass (BP) filter (Semrock, BrightLine Fluorescence Filter 425/30), angle tuned so as to pass 400 nm. A neutral density (ND) filter wheel is used to attenuate the 400 nm laser power to 25 mW, measured immediately after the filter wheel. The 400 nm beam is expanded by a factor of two and passed through an angle-tuned 440 nm shortpass (SP) filter (Semrock BrightLine Fluorescence Filter 440/SP). This filter blocks the residual 800 nm light not removed by the first filter and also functions as a dichroic mirror for bringing in either a 543 nm or a 633 nm beam from a GreNe or a HeNe laser. These beams are aligned to be collinear to the 400 nm beam and are used for initial alignment of the custom-built microscope.

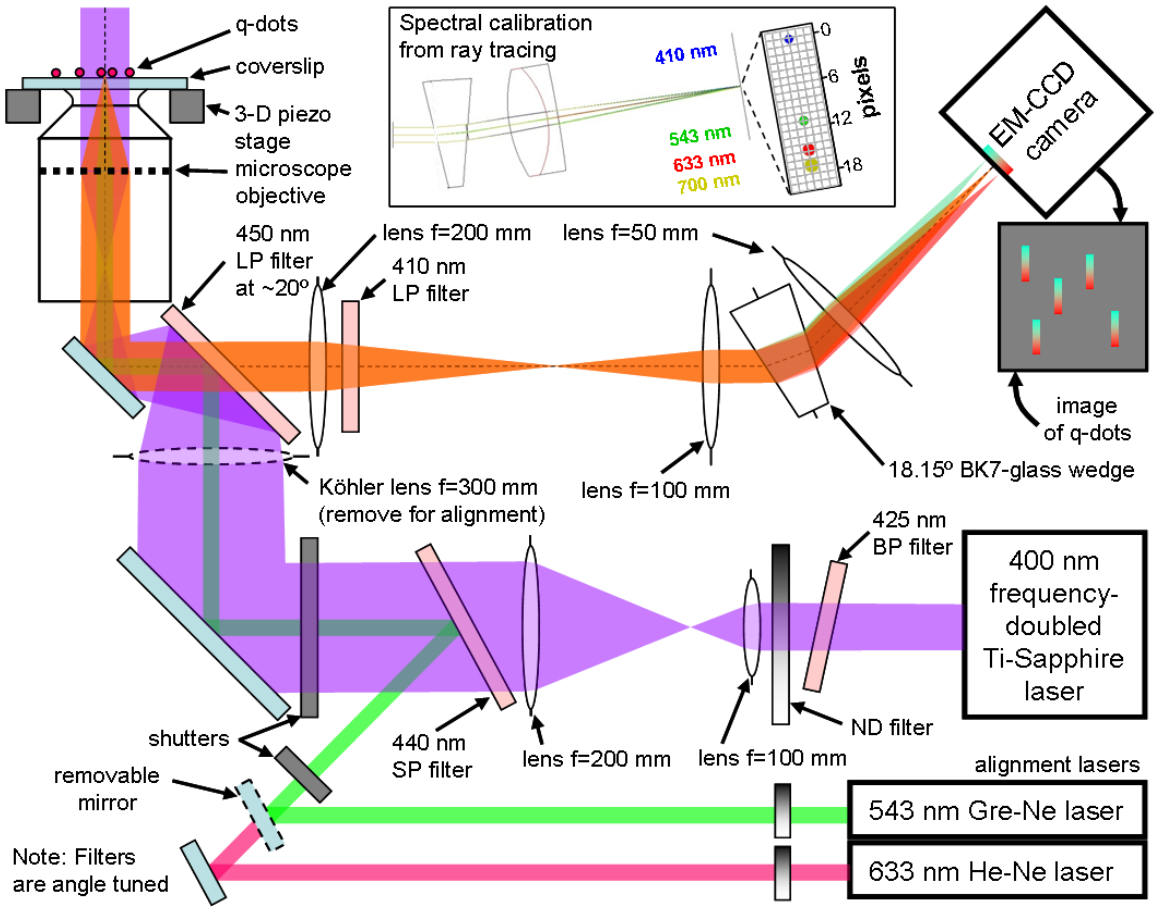

Figure 5.2: A schematic of the single-nanocrystal spectroscopy instrument. The 400 nm beam from a frequency-doubled Ti-Sapphire laser (shown in purple) is used for wide-field epi-illumination of a sample of CdSe nanocrystals. The emission from these is imaged onto a camera through a BK-7 glass wedge, which spectrally disperses the fluorescence in one dimension. The inset at top center shows ray tracing calculations, from which the spectral calibration is determined. Light in the spectral band of 410 nm – 700 nm is dispersed in one dimension over 17 camera pixels. Beams from 543 nm or 633 nm lasers are used for initial alignment of the custom-built microscope and to check the spectral calibration.

The 400 nm beam passes through a motorized shutter, which is closed to prevent photobleaching until just prior to data collection, then through a 300 mm focal length Köhler lens for wide-field illumination of the sample, and then is reflected from a 450 nm longpass (LP) filter (Omega Optics, 3RD4500LP) to the microscope objective. The LP filter, which acts as a dichroic mirror, is angle tuned to ~20º resulting in 90%

transmission at 450 nm. The objective (Olympus, 60×, water immersion, 1.2 NA, ∞/0.13-0.21, FN 2.65, model: UPlanSApo), which has an effective focal length of 3 mm and pupil diameter of 7.2 mm, was rigidly mounted to produce an inverted microscope. Focusing is achieved by lowering the coverslip to the objective with a 3D piezo stage (Thor Labs, MAX301). Prior to the Köhler lens, the 400 nm beam has a diameter of ~ 1 cm. The Köhler lens focuses the beam within the microscope objective to a point about 6 mm below the coverglass so that the objective approximately recollimates the beam at the sample to produce an illumination disk of ~100 μm diameter.

Fluorescence collected by the objective passes through the dichroic, several lenses, a glass wedge (explained below), and a 410 nm LP filter (Omega Optics, 3RD410LP), which removes the residual 400 nm scattered excitation light that passes through the dichroic. The objective would produce a magnification of 60× if used in an Olympus microscope with tube-lens focal length of 180 mm, but here the fluorescence passes through lenses with focal lengths of 200 mm, 100 mm, and 50 mm, and hence the magnification for spatial imaging is 33.3 (60 × 200/180 × 50/100). Ultrasensitive fluorescence imaging is achieved by use of an electron-multiplier charge-coupled device (EM-CCD) camera with a back-thinned sensor for high quantum-efficiency detection (Andor iXon^{EM}+, model: DU-897E-CSO-#BV). The pixel size of the camera is 16 μm, hence each pixel images a square sample area of 0.48 μm length and the 100 μm diameter illuminated sample region fills a region of ~200 camera pixels in diameter.

Initial experiments to image single nanocrystals were performed using an experimental setup without the glass wedge. Based on the observed signal strength in these experiments, it was decided to study the spectral features of single nanocrystals by

simultaneously imaging a field of many individuals using relatively low spectral dispersion/resolution, so as to achieve adequate signal-to-noise at each camera pixel. Hence a wedge made from relatively low dispersion BK7 glass, with an apex angle of 18.15° (Thorlabs PS814-A, AR Coating 350—700 nm) was chosen to disperse the emission. As seen in the inset at the top of Figure 5.2, ray tracing calculations using Zemax optical design software indicate that wedge disperses the spectral region from 410 to 700 nm over 17 camera pixels. The Airy disk diameter is 18 microns, approximately one camera pixel, consistent with experimental observations. The wedge is set at the symmetric condition of the angle of minimum deviation using the 543 nm green HeNe (GreNe) alignment laser. For alignment, the Köhler lens is removed so that the GreNe laser beam is focused to the top surface of the coverslip and the reflected portion is recollimated by the objective and passes back through the dichroic toward the wedge. After alignment of the lenses and wedge, the GreNe beam is attenuated and imaged onto the camera. The spectral dispersion is checked by replacing the 543 nm beam with the 633 nm alignment laser beam and noting the separation of the focal positions.

5.3 Spectroscopy of a Single White-Light Emitting CdSe Nanocrystal

The emission spectra of 252 nanocrystals, from five separate batches, were measured. As shown in Figure 5.3, 216 (85%) of the nanocrystals measured were individual white-light emitting CdSe nanocrystals. The remaining nanocrystals were either white-light emitting aggregates (15 measured aggregates) or monochromatic outliers (21 measured outliers). The only nanocrystals observed to not have the broad-band emission were the monochromatic outliers. All of the broad emitting nanocrystals,

aggregates and individual, span the entire spectrum. Nanocrystals that did not exhibit fluorescence intermittency were classified as aggregates. When a nanocrystal was observed to blink, the signature of single nanocrystal emission,[27,29,82] the intensity at each pixel across the row for the blinking nanocrystal was recorded. The blinking nanocrystals observed here were dispersed over 15 pixels, or ~250 nm. When a nanocrystal was observed to blink in the movie, the intensity of each pixel was recorded starting at the red edge of the emission and spanning the visible spectrum toward the blue. Each collected spectrum was 18 pixels wide and a single pixel tall. The collected spectra are from a single 50 ms frame. When the spectra were analyzed, the onset of blue emission was assumed to be 450 nm (this wavelength is the wavelength of the first emission peak in the ensemble spectrum). Previous work has shown that this peak in the white light-emission spectrum is pinned.[50] Any emission below 450 nm is likely noise.

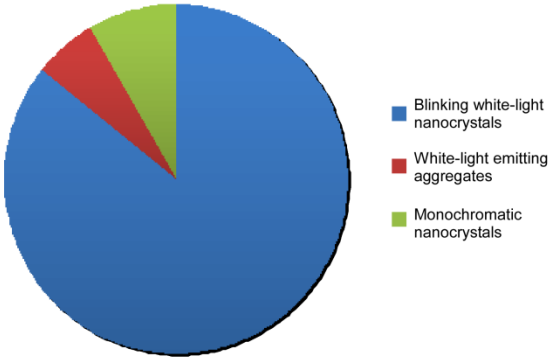

Figure 5.3: Pie chart showing the types of nanocrystals measured. The 216 blinking white-light emitting nanocrystals are shown in blue. The 15 measured white-light aggregates are shown in red. The 21 measured monochromatic outliers are shown in green.

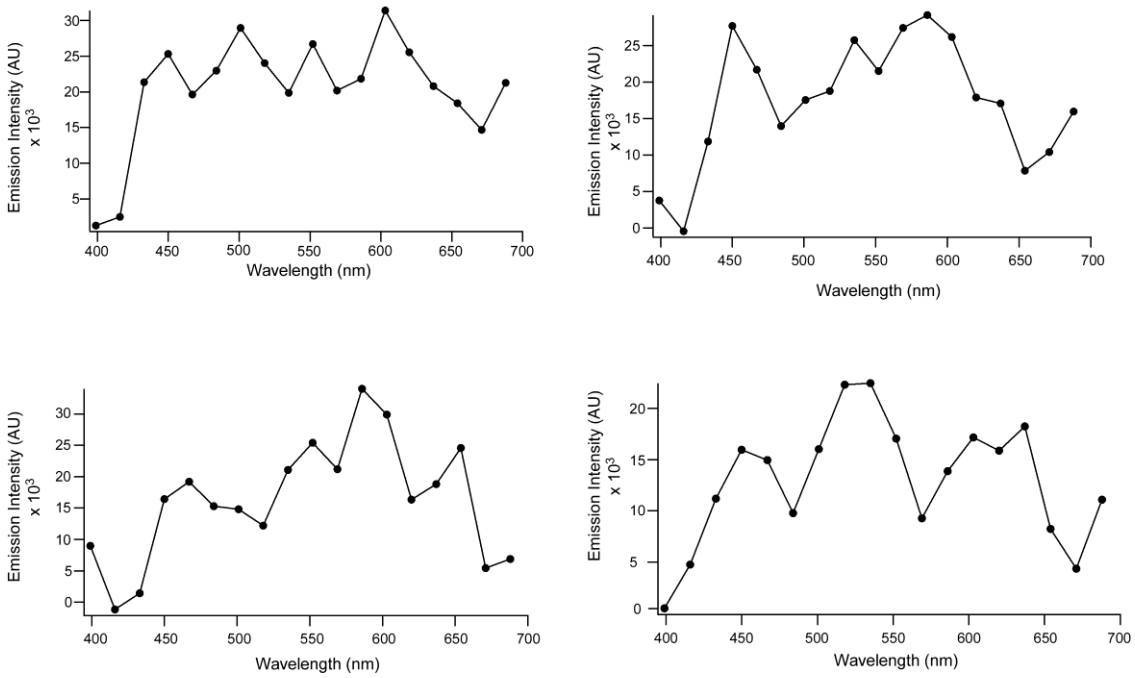

Figure 5.4: Emission spectra of selected individual white-light emitting nanocrystals. The broad emission spectrum of four different individual white-light emitting CdSe nanocrystals is shown. The wavelength of each circle on the graph is the center wavelength for each pixel, and has been connected by straight lines for clarity.

Several representative spectra are shown in Figure 5.4. While the spectra are noisy due to the small number of photons that can be collected from a single nanocrystal, it is clear that the individual nanocrystals have broad white-light emission. The observation of broad emission from individual white-light emitting CdSe nanocrystals demonstrates that the trap states responsible for the emission are uniformly distributed to each nanocrystal. Figure 5.5 shows the summation of all 216 individual emission spectra. This combined emission spectrum resembles the measured ensemble spectrum shown in Figure 5.1. Further, this implies that each white-light emitting CdSe nanocrystal has essentially the same structure. A trap state involving the surface passivating ligand has previously been shown to be responsible for the blue emission peak.[50,70] The red emission peak resembles deep-trap emission, which is the result of dangling bonds on

surface Se atoms.[74] The green (488 nm emitting) peak has been shown to be insensitive to ligand exchanges which involve ligands that bind to surface Cd atoms.[50] This suggests that surface Se atoms are also involved in the process that leads to the green emission peak.[18,50] Previous work by Bowers *et al.* determined that the decay of the population responsible for the blue peak resulted in the population of the state responsible for the red emission.[18] Bowers *et al.* observed a multi-component decay which when observed over the 50 ms integration of this work results in white light-emission from an individual CdSe nanocrystal. As shown in Figure 5.6, most of the nanocrystals are only on for one frame at a time. The intensity of the spectrum changes slightly from frame to frame, but the overall shape of the spectrum remains unchanged.

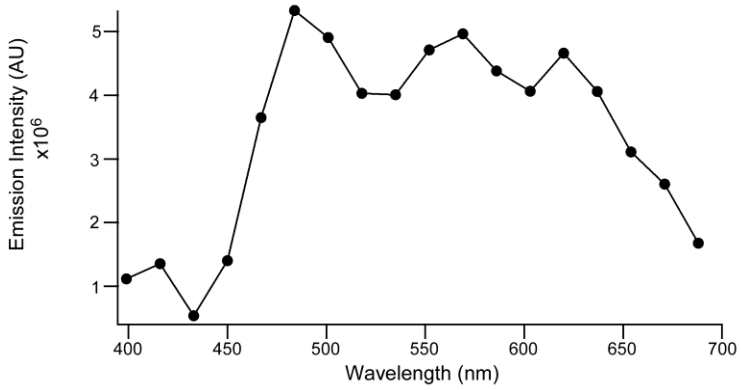

Figure 5.5: Composite emission spectrum of all individual white-light nanocrystals measured. A composite emission spectrum of the 216 individual emission spectra measured is shown. The wavelength of each circle on the graph is the center wavelength for each pixel, and has been connected by straight lines for clarity.

One of the limitations of the configuration of the instrument is its inability to establish the exact position of each nanocrystal whose spectrum is recorded. Monochromatic nanocrystals appear as single bright points on the camera. Since all the collected fluorescence passes through the wedge, and the nanocrystals are randomly

distributed onto the coverslip, it would not be possible to determine the color of two different monochromatic nanocrystals. In order to establish the color of two different monochromatic emitters, an image of scattered light of a single wavelength would need to be collected from each emitter. The displacement on the camera between the scattered light image and the fluorescent image could be calculated, and then the color could be determined. Because the CdSe nanocrystals used in this study are much smaller than the wavelength of visible light, this was not possible. It is very likely, however, that these outliers are blue emitters because CdSe nanocrystals of similar size have been reported to have blue emission.[6]

Previous studies have shown that the fluorescence spectrum of individual nanocrystals blueshift over time, which has been attributed to photo-oxidation of the nanocrystal.[27,31] We were not able to observe such a blueshift in the white-light emitting CdSe nanocrystals due to the limited spectral resolution of the experiment. Prior work showing that the emission spectrum of the ultrasmall CdSe nanocrystals is size-independent suggests that the emission spectrum should not blueshift with photo-oxidation.[50]

5.4 Blinking of White-Light Emitting CdSe Nanocrystals

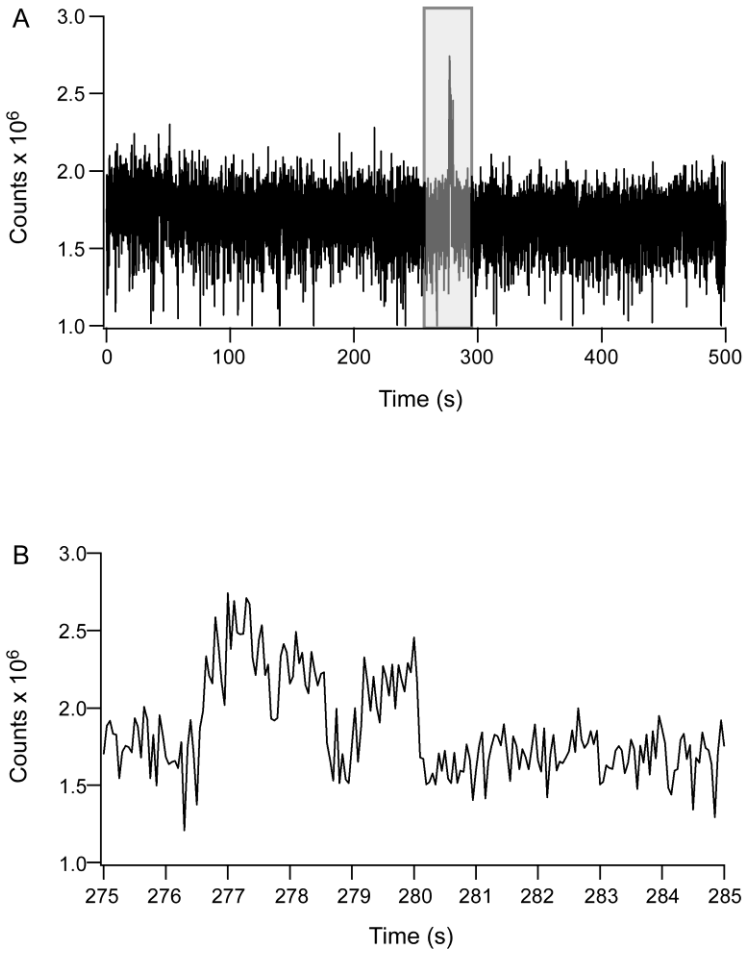

Figure 5.6: Fluoresence intensity vs. time of an individual white-light emitting CdSe nanocrystal. (A) The fluorescence intensity vs. time for a single white-light emitting CdSe nanocrystal. Data were collected for 500 seconds at 50 ms intervals. The ON state is highlighted in the gray box, which is expanded in (B).

The integrated fluorescence signal as a function of time for a single white-light emitting CdSe nanocrystals is shown in Figure 5.6. The white-light emitting CdSe nanocrystals are in the OFF state much of the time, much longer than has been reported for larger, monochromatic nanocrystals.[27,30] The extremely short ON times, shown in Figure 5.7, can be explained in the context of the Auger ionization model proposed by Nirmal *et al*.[27] Fluorescence intermittency is the result of the nanocrystal emitting in a

charge neutral state (ON) and then transitioning to a charged state (OFF).[27] Nirmal *et al*. have previously proposed a two-step ionization mechanism.[27] In the first step, a carrier becomes trapped on the nanocrystal surface. In the second step, the carrier is lost through photo-ionization within the trap state lifetime. Due to their extremely small diameter of 1.6 nm (as determined from the absorption spectrum),[45] the white-light emitting CdSe nanocrystals have a very high surface-to-volume ratio. Previous studies have estimated that as many as 70% of the atoms in a white-light emitting nanocrystal are surface atoms, compared to 22% of the atoms located at the surface of 4 nm diameter nanocrystals.[18] The resulting high concentration of surface trap states means that these states will quickly become populated. This will lead to a large population of carriers that can be photo-ionized and yield a charged (dark) nanocrystal in the OFF state.

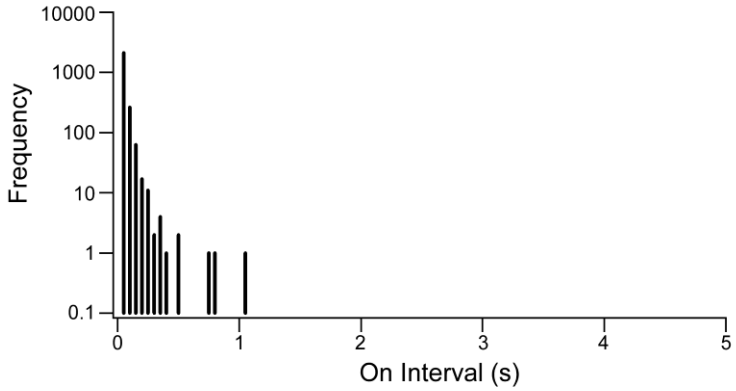

Figure 5.7: Histogram of the frequency of ON times for individual white-light CdSe nanocrystals. The histogram shows the frequency of the observed duration of the ON times for blinking white-light nanocrystals.

5.5 Conclusions about Single Nanocrystal Spectroscopy of an Individual White-Light Emitting CdSe Nanocrystal

We have shown that the emission of individual white-light emitting CdSe nanocrystals is white. The white-light emitting CdSe nanocrystals were observed to blink with all wavelengths emitting simultaneously. The nanocrystals are in a non-emitting state the majority of the time. This is the result of the extreme surface-to-volume ratio that leads to a high density of non-radiative surface trap states. This work shows that the trap states responsible for the white-light emission are present on each white-light emitting CdSe nanocrystal.

CHAPTER VI

CONCLUSIONS AND FUTURE DIRECTIONS

6.1 Overall Conclusions

In traditional CdSe nanocrystals both the band edge absorption and band edge emission blue shift with decreasing crystal diameter. This trend no longer holds for ultrasmall CdSe nanocrystals. The blue peak in the emission spectrum was observed to become size independent or pinned at nanocrystal diameters of 1.7 nm and smaller. As the diameter of the nanocrystal was increased the emission spectrum was observed to change from the broad white-light emission spectrum to a narrow monochromatic emission spectrum as soon as the nanocrystal diameter is no longer in the pinned emission size régime. Additionally, ligand exchange reactions were performed on ultrasmall nanocrystals with pinned emission to replace the alkylphosphonic acid ligands with oleic acid, pyridine, or dodecanethiol. In each case the pinned emission peak was quenched, indicating that the surface alkylphosphonic acid ligand is responsible for the pinned emission. We propose that this trap state has a fixed energy and is always present in CdSe nanocrystals, however; the trap state is typically higher in energy than the conduction band for larger nanocrystals and is not observed. Pinned emission only becomes observable when the band gap increases at extremely small nanocrystal diameters. Since the trap state responsible for the pinned emission is ligand dependent, choosing a different ligand should result in the emission being pinned at a different wavelength.

Single nanocrystal fluorescence spectroscopy has been performed on individual white-light emitting nanocrystals to determine if the white-light emission is the result of an ensemble effect. These measurements showed that each white-light emitting nanocrystal emits white-light on the timescale of the integration (50 ms). The white-light emission spectrum is the result of several different trap states emitting simultaneously. These single nanocrystal measurements indicate that each white-light emitting nanocrystal has all of the trap states necessary for white-light emission. The blue peak is the result of trap state emission at the dodecylphosphonic acid ligand, while the red emission peak is the result of deep trap recombination at the surface Se atoms. The white-light emitting nanocrystals were observed to blink. The blinking is uniform, *i.e.* the blue, green, and red peaks blink together on the time scale of the measurement (50 ms).

Changing the surface ligand used in the nanocrystal synthesis from dodecylphosphonic acid to diisooctylphosphinic acid results in quantized growth of the absorption spectrum. Quantized growth is the hallmark of magic-sized nanocrystals. The steric effects from the secondary phosphinic acid ligand result in decreased emission from band edge absorption. By varying the synthetic conditions it was determined that both a strongly coordinating solvent (hexadecylamine) and a strongly binding ligand (diisooctylphosphinic acid) are necessary to synthesize magic-size nanocrystals. It was also observed that as magic-size nanocrystals grow to a larger size a morphological change was observed in transmission electron micrographs. The use of diisooctylphosphinic acid has been shown to yield larger magic-sized nanocrystals than previously reported synthesis.

6.2 Future Directions

While a morphological change was observed in the TEM images of the magic-size nanocrystals, a lattice resolved image was not obtained. In order to determine if the structure proposed by Kasuya *et al.* is correct a lattice resolved image is necessary. Scanning transmission electron microscopy (STEM) has subangstrom resolution which is superior to the resolution of TEM. If the proposed cluster-cage model can be shown with STEM imaging it would demonstrate a crystal structure which is unique to nanomaterials.

Individual white-light emitting CdSe nanocrystals were observed to blink, however a detailed study of the blinking statistics has yet to be completed. A thorough study of the blinking statistics will determine if white-light nanocrystals show the same inverse power law behavior observed in larger nanocrystals. Because the white-light emission spectrum is dominated by trap state recombination rather than band edge electron-hole recombination, their blinking statistics may be significantly different. If the blinking statistics do not follow the inverse power-law behavior then a different mechanism may be responsible for the observed blinking in white-light nanocrystals.

The white-light emission spectrum is the result of several different surface-trap states. While the blue and red peaks appear to be understood, attempts to modify the green peak (488 nm emission) have been unsuccessful. Post-preparative ligand exchanges affect only the surface Cd atoms and change the blue peak, while the green peak remains unchanged. It is thought that the green peak is the result of recombination at a Se atom; however it is not clear if this is a surface or interior Se atom. If any of the surface states is altered, the white-light emission spectrum is degraded. This rules out traditional methods of increasing the fluorescence quantum yield such as shelling with a

wider band gap material like ZnS. The shell material would eliminate the surface traps necessary for the white-light emission. Most research has focused on eliminating trap states, but to increase the quantum yield of the white-light nanocrystals will require new methods be developed which enhance trap state recombination.

APPENDIX A

CHROMATOGRAPHY OF WHITE-LIGHT CDSE NANOCRYSTALS

A.1 Separating Excess Starting Material from CdSe Nanocrystals

One often overlooked aspect of the synthesis of semiconductor nanocrystals is the need to remove excess starting material from the final product. When the synthesis of CdSe nanocrystals relied on $CdMe_2$ as the cadmium precursor, repeated precipitation and collection of the nanocrystals by centrifugation (detailed in Chapter II) was sufficient to obtain a sample free of excess starting material.[4,66] Using this synthetic technique Taylor *et al.* were able to establish the Cd:Se ratio in CdSe nanocrystals as 1.2:1.[66] With the $CdMe_2$ synthesis, the unreacted precursors which need to be removed are trioctylphosphine oxide (TOPO), Cd, Se, and tributylphosphine (TBP). The TOPO and TBP will dissolve in methanol and while the nanocrystals and the metals will precipitate. Three washes with were required to obtain clean nanocrystals.[66,73]

As the synthesis of nanocrystals evolved to the use of CdO and dodecylphosphonic acid to generate a reactive cadmium precursor, the cleanup process for removing excess starting material changed.[18,50,51] Instead of precipitating from methanol three times, CdSe nanocrystals are precipitated from methanol, then dissolved in hexanol or octanol which precipitates Cd salts, then the nanocrystals are precipitated with methanol and dispersed in solvent for use. However, since the reactive cadmium precursor is a cadmium phosphonate, its chemical similarity to the surface of the nanocrystal could make it more difficult to remove by the simple precipitation and

centrifugation traditionally employed. This results in a higher Cd:Se ratio than the 1.2:1 that was observed by Taylor *et al.*[66]

A.2 Column Chromatography of White-Light Emitting Nanocrystals

White-light emitting CdSe nanocrystals are synthesized as previously described in Chapter II.[10] Chromatography was performed with silca gel as the stationary phase. The dirty nanocrystal solution is applied directly to the column once it has cooled below 100 °C. Hexanes was used as the mobile phase because the nanocrystals are soluble in hexanes while the Cd salts are not as soluble. Figure A.1 shows a typical chromatography set up, but with larger nanocrystals instead of white-light nanocrystals. Under room light (Fig. A.1 A) the nanocrystals appear evenly distributed through the silica gel. However, under UV illumination (Fig. A.1 B) it becomes obvious that most of the nanocrystals are retained at the top of the column.

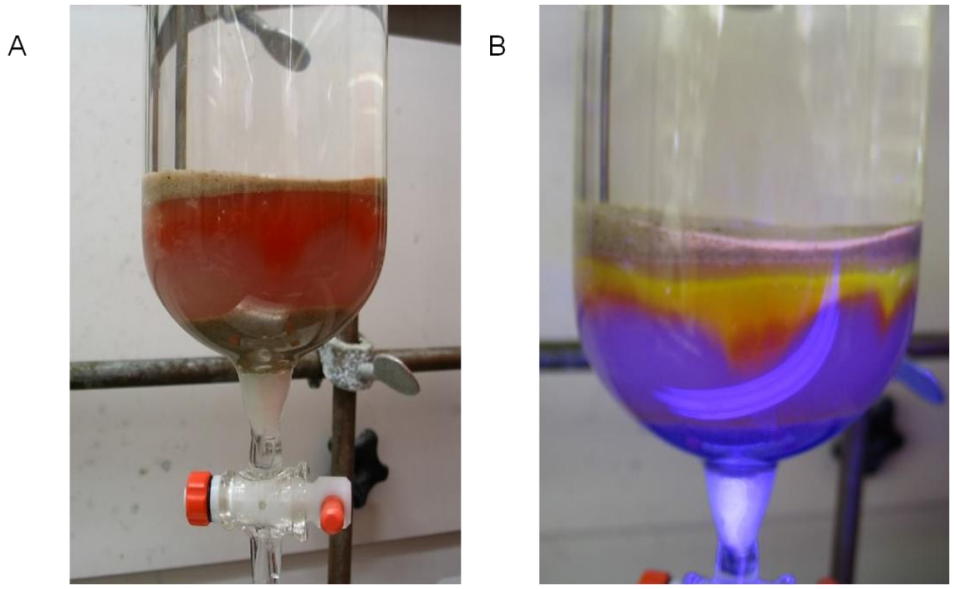

Figure A.1: Photograph of nanocrystal chromatography setup. (A) Chromatography column after nanocrystal separation under room light. (B) Chromatography separation of nanocrystals under UV light.

A.3 Cd:Se Ratio in White-Light Emitting CdSe Nanocrystals

Rutherford backscattering spectroscopy (RBS) was used to determine the Cd:Se ratio in white-light emitting CdSe nanocrystals, and is shown in Figure A.2. White-light emitting CdSe nanocrystals which were cleaned using the traditional precipitation and centrifugation method are shown in blue. Typically, this cleanup yields nanocrystal samples which have a Cd:Se ratio of ~4:1 or higher. This is much higher than should be expected based on Taylor et al. previous work.

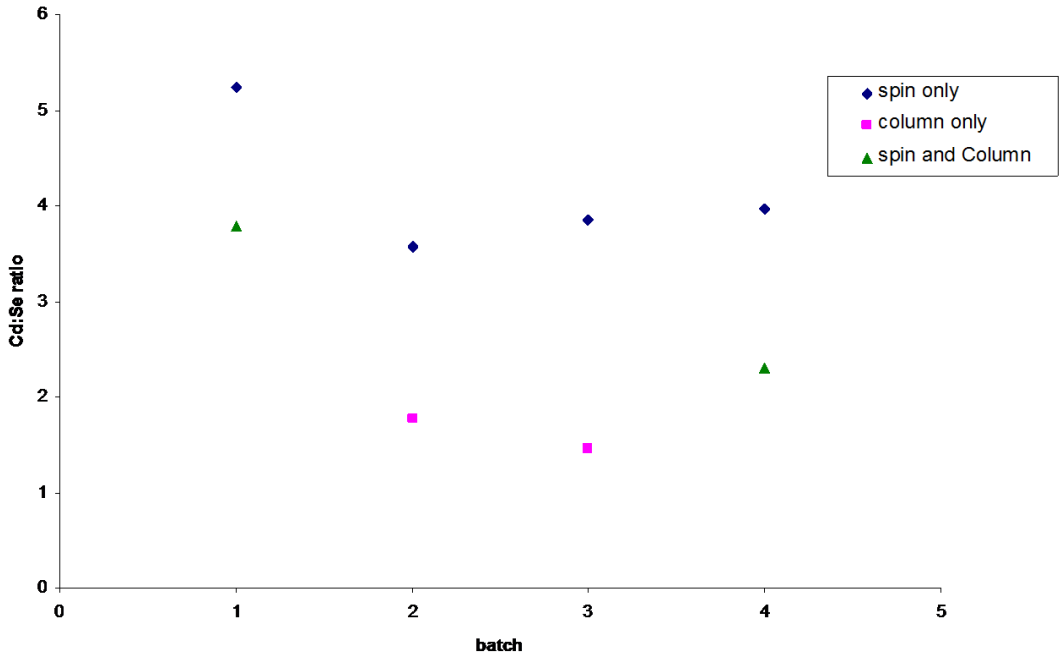

Figure A.2: Cd:Se ratio for various cleaning methods. The Cd:Se ratio was determined by RBS for white-light emitting nanocrystals which were cleaned by various methods. The traditional precipitation method is labeled spin only and is shown in blue. Cleaning by column chromatography with silca gel is shown in pink, while samples cleaned by both precipitation and chromatography are shown in green.

To test if column chromatography using silca gel does a better job of removing precursors than the traditional precipitation clean up, the Cd:Se ratio was measured for the same batch of nanocrystals cleaned using each method. After synthesis, half the batch would be passed through the column, while the other half would be cleaned via precipitation. The results of column chromatography in Figure A.2 are shown in pink, the Cd:Se ratio for these samples is ~2:1. While this is still higher than the Cd:Se ratio reported by Taylor, it is much lower than the Cd:Se ratio obtained for precipitation only.

When chromatography was combined with precipitation (green in Figure A.2), the Cd:Se ratio was also observed to be lower than precipitation only. While the chromatography does remove more of the unreacted Cd salts from the nanocrystal solution, RBS measurements show that there are likely still excess Cd salts in the solution.

A.4 Effects of Chromatography on the White-Light Emission Spectrum

Using column chromatography to remove excess Cd salts does alter the white-light emission spectrum as shown in Figure A.3. The deep trap emission peak increases in intensity and redshifts slightly after the nanocrystals have passed through the column. The chromatography conditions do not alter the blue emission peak position or intensity, while the green peak, at 488 nm, appears to increase slightly in intensity. The increase to the green peak is likely the result of the dramatic increase in the deep trap peak spilling over to this region of the spectrum. Because the slica gel is acidic the increase in intensity of the deep trap peak is likely the result of surface oxidation as the nanocrystals pass through the column.

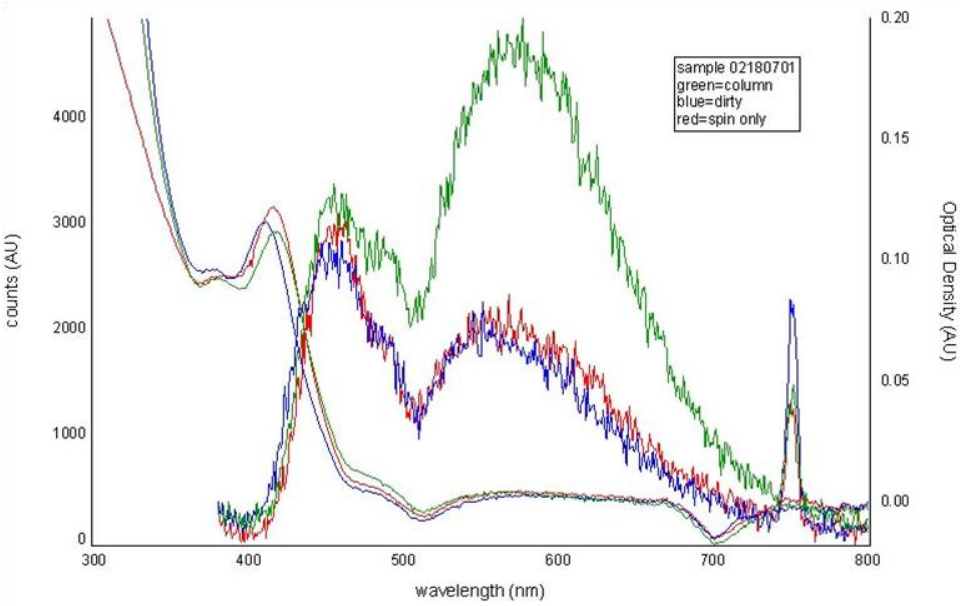

FigureA.3: Absorption and emission of cleaned and dirty nanocrystals. The absorption and emission of white-light CdSe nancorystals is shown above. The dirty nanocrystals are shown in blue. The absorption and emission of the nanocrystals after precipitation cleaning is shown in red. The absorption and emission of chromatography cleaned nanocrystals are shown in green.

The chromatography column clean up method also results in an increase in the fluorescent quantum yield of the white-light nanocrystals as shown in Figure A.4. The precipitation clean up also increases the fluorescent quantum yield over the dirty nanocrystals, but not as much as the chromatography clean up. The dirty nanocrystals have a quantum yield of ~4 %, while the nanocrystals cleaned by precipitation have a quantum yield of ~6 %. The nanocrystals cleaned up via chromatography have a quantum yield of ~9 %, a 33% improvement over the precipitation method.

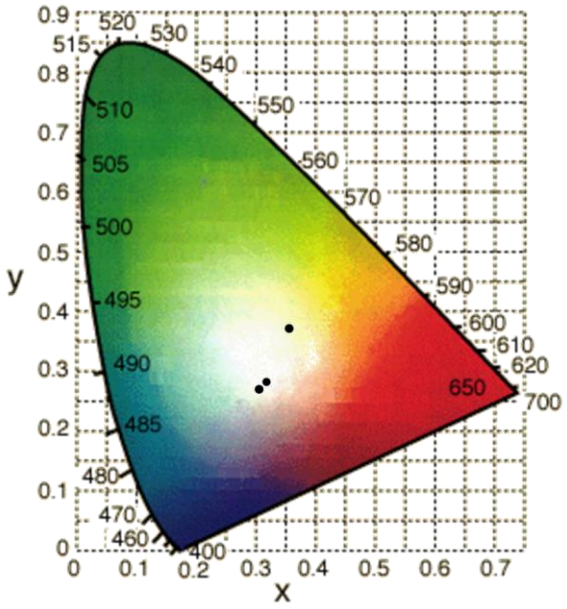

Figure A.4: CIE coordinates of clean and dirty nanocrystals. 1931 CIE coordinates for white-light nanocrystals dirty (0.299, 0.307), precipitation clean up (0.312, 0.317), and chromatography clean up (0.369, 0.382).

1931 CIE coordinates are mathmatical method for determining how the average human eye will precieve a color.[83] Pure white in the 1931 CIE coordinates is (0.333, 0.333). As synthesized the dirty white-light nanocrystals have 1931 CIE coordinatres of (0.299, 0.307), and clean up by precipitation does not signifcantly alter the CIE coordinates to (0.312, 0.317) as shown in Figure A.4. However, the signifcant increase in the deep trap emission that results from chromatography clean up shifts the CIE coordinates signifcantly to (0.369, 0.382). This shift raises the posiblity that chromatography could also be useful in tuning the white-light nanocrystals emission spectrum. Previous work on altering the white-light emission spectrum has centered on altering the blue emission peak.[70,81,84] Enhancing the red emission peak results in a warm white emission, which is more appealing to the American lighting market.

REFERENCES

(1) Fahlman, B. D. *Materials Chemistry*; 1st ed.; Springer: Mount Pleasant, MI, 2007; Vol. 1.

(2) Brus, L. E. *J. Chem. Phys.* **1984**, *80*, 4403.

(3) Chestnoy, N.; Harris, T. D.; Hull, R.; Brus, L. E. *J. Phys. Chem.* **1986**, *90*, 3393.

(4) Murray, C. B.; Norris, D. J.; Bawendi, M. G. *J. Am. Chem. Soc.* **1993**, *115*, 8706.

(5) McBride, J. R.; Dukes III, A. D.; Schreuder, M. A.; Rosenthal, S. J. *Chem. Phys. Lett.* **2010**, *498*, 1.

(6) Ouyang, J.; Zaman, M. B.; Yan, F. J.; Johnston, D.; Li, G.; Wu, X.; Leek, D.; Ratcliffe, C. I.; Ripmeester, J. A.; Yu, K. *J. Phys. Chem. C* **2008**, *112*, 13805.

(7) Kudera, S.; Zanella, M.; Giannini, C.; Rizzo, A.; Li, Y. Q.; Gigli, G.; Cingolani, R.; Ciccarella, G.; Spahl, W.; Parak, W. J.; Manna, L. *Adv. Mater.* **2007**, *19*, 548.

(8) Kasuya, A.; Sivamohan, R.; Barnakov, Y. A.; Dmitruk, I. M.; Nirasawa, T.; Romanyuk, V. R.; Kumar, V.; Mamykin, S. V.; Tohji, K.; Jeyadevan, B.; Shinoda, K.; Kudo, T.; Terasaki, O.; Liu, Z.; Belosludov, R. V.; Sundararajan, V.; Kawazoe, Y. *Nat. Mater.* **2004**, *3*, 99.

(9) Dagtepe, P.; Chikan, V.; Jasinski, J.; Leppert, V. J. *J. Phys. Chem. C* **2007**, *111*, 14977.

(10) Bowers, M. J.; McBride, J. R.; Rosenthal, S. J. *J. Am. Chem. Soc.* **2005**, *127*, 15378.

(11) Jose, R.; Zhelev, Z.; Bakalova, R.; Baba, Y.; Ishikawa, M. *Appl. Phys. Lett.* **2006**, *89*, 013115.

(12) Landes, C. F.; Braun, M.; El-Sayed, M. A. *J. Phys. Chem. B* **2001**, *105*, 10554.

(13) Soloviev, V. N.; Eichhofer, A.; Fenske, D.; Banin, U. *J. Am. Chem. Soc.* **2001**, *123*, 2354.

(14) Chen, X. B.; Samia, A. C. S.; Lou, Y. B.; Burda, C. *J. Am. Chem. Soc.* **2005**, *127*, 4372.

(15) Landes, C.; Braun, M.; El-Sayed, M. A. *Chem. Phys. Lett.* **2002**, *363*, 465.

(16) Landes, C.; El-Sayed, M. A. *J. Phys. Chem. A* **2002**, *106*, 7621.

(17) Landes, C.; Braun, M.; Burda, C.; El-Sayed, M. A. *Nano Lett.* **2001**, *1*, 667.

(18) Bowers, M. J.; McBride, J. R.; Garrett, M. D.; Sammons, J. A.; Dukes, A. D.; Schreuder, M. A.; Watt, T. L.; Lupini, A. R.; Pennycook, S. J.; Rosenthal, S. J. *J. Am. Chem. Soc.* **2009**, *131*, 5730.

(19) Landes, C.; Burda, C.; Braun, M.; El-Sayed, M. A. *J. Phys. Chem. B* **2001**, *105*, 2981.

(20) El-Sayed, M. A. *Accounts Chem. Res.* **2004**, *37*, 326.

(21) Tolbert, S. H.; Alivisatos, A. P. *Science* **1994**, *265*, 373.

(22) Zanella, M.; Abbasi, A. Z.; Schaper, A. K.; Parak, W. J. *J. Phys. Chem. C* **2010**, *114*, 6205.

(23) Pedersen, J.; Bjornholm, S.; Borggreen, J.; Hansen, K.; Martin, T. P.; Rasmussen, H. D. *Nature* **1991**, *353*, 733.

(24) Choi, H. S.; Liu, W.; Misra, P.; Tanaka, E.; Zimmer, J. P.; Ipe, B. I.; Bawendi, M. G.; Frangioni, J. V. *Nat. Biotechnol.* **2007**, *25*, 1165.

(25) Schreuder, M. A.; Gosnell, J. D.; Smith, N. J.; Warnement, M. R.; Weiss, S. M.; Rosenthal, S. J. *J. Mater. Chem.* **2008**, *18*, 970.

(26) Schreuder, M. A.; Xiao, K.; Ivanov, I. N.; Weiss, S. M.; Rosenthal, S. J. *Nano Lett.* **2010**, *10*, 573.

(27) Nirmal, M.; Dabbousi, B. O.; Bawendi, M. G.; Macklin, J. J.; Trautman, J. K.; Harris, T. D.; Brus, L. E. *Nature* **1996**, *383*, 802.

(28) Kuno, M.; Fromm, D. P.; Hamann, H. F.; Gallagher, A.; Nesbitt, D. J. *J. Chem. Phys.* **2000**, *112*, 3117.

(29) Kuno, M.; Fromm, D. P.; Hamann, H. F.; Gallagher, A.; Nesbitt, D. J. *J. Chem. Phys.* **2001**, *115*, 1028.

(30) Shimizu, K. T.; Neuhauser, R. G.; Leatherdale, C. A.; Empedocles, S. A.; Woo, W. K.; Bawendi, M. G. *Phys. Rev. B* **2001**, *63*, 205316.

(31) Neuhauser, R. G.; Shimizu, K. T.; Woo, W. K.; Empedocles, S. A.; Bawendi, M. G. *Phys. Rev. Lett.* **2000**, *85*, 3301.

(32) Zhao, J.; Nair, G.; Fisher, B. R.; Bawendi, M. G. *Phys. Rev. Lett.* **2010**, *104*, 157403.

(33) Mason, M. D.; Credo, G. M.; Weston, K. D.; Burrato, S. K. *Phys. Rev. Lett.* **1998**, *80*, 5405.

(34) Bopp, M. A.; Jia, Y.; Li, L.; Cogdill, R.; Hochstrasser, R. M. *Proc. Natl. Acad. Sci. U.S.A.* **1997**, *94*, 10630.

(35) Dickson, R. M.; Cubitt, A. B.; Tsien, R. Y.; Moerner, W. E. *Nature* **1997**, *388*, 355.

(36) Peterman, E. J. G.; Brasselet, S.; Moerner, W. E. *J. Phys. Chem. A* **1999**, *103*, 10553.

(37) Lu, H. P.; Xie, X. S. *Nature* **1997**, *385*, 143.

(38) Ha, T.; Enderle, T.; Chemla, D. S.; Selvin, P. R.; Weiss, S. *Chem. Phys. Lett.* **1997**, *271*, 1.

(39) Weston, K. D.; Carson, P. J.; Metiu, H.; Burrato, S. K. *J. Chem. Phys.* **1998**, *109*, 7474.

(40) Hoyer, P.; Staudt, T.; Engelhardt, J.; Hell, S. W. *Nano Lett.* **2010**, *11*, 245.

(41) Peterson, J. J.; Krauss, T. D. *Nano Lett.* **2006**, *6*, 510.

(42) Empedocles, S. A.; Neuhauser, R.; Shimizu, K.; Bawendi, M. G. *Adv. Mater.* **1999**, *11*, 1243.

(43) Li, X.-Q.; Arakawa, Y. *Phys. Rev. B* **1999**, *60*, 1915.

(44) Joo, J.; Son, J. S.; Kwon, S. G.; Yu, J. H.; Hyeon, T. *J. Am. Chem. Soc.* **2006**, *128*, 5632.

(45) Yu, W. W.; Qu, L. H.; Guo, W. Z.; Peng, X. G. *Chem. Mater.* **2003**, *15*, 2854.

(46) Garrett, M. D.; Dukes, A. D.; McBride, J. R.; Smith, N. J.; Pennycook, S. J.; Rosenthal, S. J. *J. Phys. Chem. C* **2008**, *112*, 12736.

(47) Kopping, J. T.; Patten, T. E. *J. Am. Chem. Soc.* **2008**, *130*, 5689.

(48) *March's Advanced Organic Chemistry: Reactions, Mechanisms, and Structre*; 5th ed.; Smith, M. B.; March, J., Eds.; Wiley: New York, 2001.

(49) *Organic Synthesis*; Smith, M. B., Ed.; Wiley: New York, 1994.

(50) Dukes III, A. D.; Schreuder, M. A.; Sammons, J. A.; McBride, J. R.; Smith, N. J.; Rosenthal, S. J. *J. Chem. Phys.* **2008**, *129*, 121102.

(51) Garrett, M. D.; Bowers, M. J.; McBride, J. R.; Orndorff, R. L.; Pennycook, S. J.; Rosenthal, S. J. *J. Phys. Chem. C* **2008**, *112*, 436.

(52) Jose, R.; Zhanpeisov, N. U.; Fukumura, H.; Baba, Y.; Ishikawa, M. *J. Am. Chem. Soc.* **2006**, *128*, 629.

(53) Sapra, S.; Mayilo, S.; Klar, T. A.; Rogach, A. L.; Feldmann, J. *Adv. Mater.* **2007**, *19*, 569.

(54) Jose, R.; Zhelev, Z.; Bakalova, R.; Baba, Y.; Ishikawa, M. *Applied Physics Letters* **2006**, *89*.

(55) Nag, A.; Sarma, D. D. *J. Phys. Chem. C* **2007**, *111*, 13641.

(56) Puzder, A.; Williamson, A. J.; Gygi, F.; Galli, G. *Phys. Rev. Lett.* **2004**, *92*.

(57) Lee, J. R. I.; Meulenberg, R. W.; Hanif, K. M.; Mattoussi, H.; Klepeis, J. E.; Terminello, L. J.; van Buuren, T. *Phys. Rev. Lett.* **2007**, *98*.

(58) Wilcoxon, J. P.; Provencio, P. P. *J. Phys. Chem. B* **2005**, *109*, 13461.

(59) Efros, A. L.; Rosen, M.; Kuno, M.; Nirmal, M.; Norris, D. J.; Bawendi, M. *Phys. Rev. B* **1996**, *54*, 4843.

(60) Kuno, M.; Lee, J. K.; Dabbousi, B. O.; Mikulec, F. V.; Bawendi, M. G. *J. Chem. Phys.* **1997**, *106*, 9869.

(61) Rosenbaum, E. J.; Grosse, A. V.; Jacobson, H. F. *J. Am. Chem. Soc.* **1939**, *61*, 689.

(62) Munro, A. M.; Jen-La Plante, I.; Ng, M. S.; Ginger, D. S. *Journal of Physical Chemistry C* **2007**, *111*, 6220.

(63) Bullen, C.; Mulvaney, P. *Langmuir* **2006**, *22*, 3007.

(64) *CRC Handbook of Chemistry and Physics*; 83 ed.; Lide, D. R., Ed.; CRC Press: Boca Raton, 2002.

(65) Yu, W. W.; Wang, Y. A.; Peng, X. G. *Chem. Mater.* **2003**, *15*, 4300.

(66) Taylor, J.; Kippeny, T.; Rosenthal, S. J. *J. Clust. Sci.* **2001**, *12*, 571.

(67) Peng, X. G.; Manna, L.; Yang, W. D.; Wickham, J.; Scher, E.; Kadavanich, A.; Alivisatos, A. P. *Nature* **2000**, *404*, 59.

(68) Wang, W.; Banerjee, S.; Jia, S. G.; Steigerwald, M. L.; Herman, I. P. *Chem. Mater.* **2007**, *19*, 2573.

(69) Rempel, J. Y.; Trout, B. L.; Bawendi, M. G.; Jensen, K. F. *J. Phys. Chem. B* **2006**, *110*, 18007.

(70) Schreuder, M. A.; McBride, J. R.; Dukes III, A. D.; Sammons, J. A.; Rosenthal, S. J. *J. Phys. Chem. C* **2009**, *113*, 8169.

(71) Gosnell, J. D.; Schreduer, M. A.; II, M. J. B.; Rosenthal, S. J.; Weiss, S. M. *Proc. of SPIE* **2006**, *6337*, 63370A.

(72) Hoheisel, W.; Colvin, V. L.; Johnson, C. S.; Alivisatos, A. P. *J. Chem. Phys.* **1994**, *101*, 8455.

(73) Underwood, D. F.; Kippeny, T.; Rosenthal, S. J. *J. Phys. Chem. B* **2001**, *105*, 436.

(74) Pokrant, S.; Whaley, K. B. *Eur. Phys. J. D* **1999**, *6*, 255.

(75) Puzder, A.; Williamson, A. J.; Zaitseva, N.; Galli, G.; Manna, L.; Alivisatos, A. P. *Nano Lett.* **2004**, *4*, 2361.

(76) McBride, J. R.; Lupini, A. R.; Schreuder, M. A.; Smith, N. J.; Pennycook, S. J.; Rosenthal, S. J. *ACS Appl. Mater. Inter.* **2009**, *1*, 2886.

(77) Ithurria, S.; Dubertret, B. *J. Am. Chem. Soc.* **2008**, *130*, 16504.

(78) Liu, Y.-H.; Wayman, V. L.; Gibbons, P. C.; Loomis, R. A.; Buhro, W. E. *Nano Lett.* **2010**, *10*, 352.

(79) Nguyen, K. A.; Day, P. N.; Pachter, R. *J. Phys. Chem. C* **2010**, *114*, 16197.

(80) Gosnell, J. D.; Rosenthal, S. J.; Weiss, S. M. *IEEE Photonics Technology Letters* **2010**, *22*, 541.

(81) Qian, L.; Bera, D.; Holloway, P. H. *Nanotechnology* **2008**, *19*, 285702.

(82) Krauss, T. D.; Peterson, J. J. *J. Phys. Chem. Lett.* **2010**, *1*, 1377.

(83) http://www.cie.co.at/index.php/LEFTMENUE/index.php?i_ca_id=298 30 January 2011

(84) Demir, H. V.; Nizamoglu, S.; Mutlugun, E.; Ozel, T.; Sapra, S.; Gaponik, N.; Eychmuller, A. *Nanotechnology* **2008**, *19*.